N.D. Denkov, K.G. Marinova, Antifoam effects of solid particles, oil drops and oil-solid compounds in aqueous foams. Chapter 10 in the book *"Colloidal Particles at Liquid Interfaces"* (B.P. Binks & T.S. Horozov, Eds.), Cambridge University Press, Cambridge, UK, 2006; pp. 383-444.

Chapter 10

Antifoam effects of solid particles, oil drops and oil-solid compounds in aqueous foams

Nikolai D. Denkov and Krastanka G. Marinova

Laboratory of Chemical Physics & Engineering, Faculty of Chemistry, Sofia University,
1 J. Bourchier Avenue, 1164 Sofia, Bulgaria

1 Introduction

1.1 The antifoam effect

Foams appear as an integral part of various technological applications, such as ore and mineral flotation, tertiary oil recovery, production of porous insulating materials, fire fighting and many others. Foams are also encountered in certain types of consumer products, *e.g.* the mousses and ice-creams as food products and shaving and styling foams in cosmetics.[1,2] It has been known for many years that the presence of oil droplets and/or hydrophobic solid particles in the aqueous foaming solutions can strongly reduce the foaminess and foam stability, which might be a problem in various applications.[1-9] For example, the fat particles in food products and the droplets of silicone oil used in personal care products (such as shampoos and hair/skin conditioners) have a strong antifoam effect, which should be suppressed to achieve an acceptable product quality from a consumer viewpoint.

On the other hand, excessive foaming might create serious problems in many industrial processes. Typical examples are during fermentation in drug and food manufacturing, the processing of drug emulsions and suspensions, pulp and paper production, industrial water purification, beverage production and packaging, textile dyeing, oil rectification and many others.[1,4,6] That is why special additives called "antifoams" or "defoamers" are widely used in these and other industrial applications to suppress foam formation or to destroy already formed foam.[1,3-9] The antifoams are also indispensable components of several everyday commercial products, such as washing machine detergents, paints and anti-flatulence drugs.[4]

We illustrate the antifoam effect in Figure 10.1 by showing the foam volume *versus* time, $V_F(t)$, for foam generated from a micellar solution of anionic surfactant AOT (sodium bis-2-ethylhexylsulphosuccinate) in the presence of 0.01 wt. % of two different antifoams – silicone oil and a compound of silicone oil + hydrophobized silica particles. One sees that the reference foam (in the absence of antifoam) is stable, whereas the two antifoams lead to relatively rapid foam decay; note the different manner of foam destruction by the two antifoams. The silicone oil does not affect the foaminess of the solution and the foam destruction starts only after an initial induction period, lasting for about 1 minute after the foaming agitation was stopped. The main course of foam destruction continues for an additional 2 minutes and, afterwards, the residual foam remains stable for tens of minutes. In contrast, the oil+particle compound significantly reduces the foaminess of the AOT solution and destroys the foam completely in less than 20 seconds. These different patterns of foam destruction are related to two different modes of antifoam action,[8,10-25] which are explained in section 2.3 and are discussed throughout this chapter.

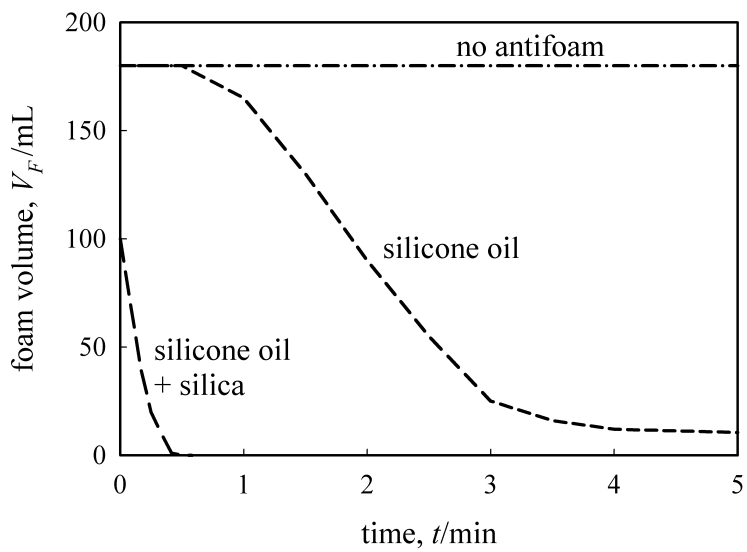

Figure 10.1. Foam volume V_F *versus* time t for foam generated by 10 hand-shakes (Bartsch test) from a 10 mM solution of the anionic surfactant AOT in the absence of antifoam and in the presence of 0.01 wt. % of two different antifoams - silicone oil or a compound of silicone oil + hydrophobized silica particles. Adapted from ref. 22.

Various terms are used to characterize the antifoam performance. The activity of antifoams characterizes their ability to prevent foam generation during agitation and/or to destroy rapidly pre-generated foams. Thus higher antifoam activity means less generated foam and/or faster foam destruction.[3-9] The antifoam exhaustion (deactivation) is a process in which the antifoam loses its activity in the course of foam destruction.[5-8,12,19-21,24-28] The durability of an antifoam characterizes its ability to destroy a larger total amount of foam before exhaustion, or to maintain the instantaneous foam volume below a specified value (during continuous foaming) for a longer period of time.[8,12,19-21,24,25] Finally, the term antifoam efficiency is used to characterize the antifoam in a general sense, with respect to both activity and durability.

The meaning of these terms is illustrated in Figure 10.2, which shows the effect of an antifoam compound on the foam evolution in the Foam Rise test.[8,20,25] In this method, a controlled flux of nitrogen gas is continuously blown through a parallel set of glass capillaries and the dependence $V_F(t)$ is monitored. As seen from Figure 10.2, the increase in the foam volume is very fast in the absence of antifoam. In contrast, when only 0.02 wt. % of oil+silica particle compound was pre-dispersed in the foaming solution, the foam volume remained below 10 mL for about 50 minutes, as a result of the rapid rupture of the foam bubbles by the antifoam. After this initial stage of low foam volume being maintained (stage 1), a sudden, almost complete loss of the antifoam activity is observed - see the rapid foam growth during stage 2 in Figure 10.2. The sharp break in the curve $V_F(t)$, denoted by t_{EX}, indicates the moment of antifoam exhaustion, when the process of bubble destruction by the antifoam becomes too slow to compensate for the bubble generation. The total volume of the foam destroyed by the antifoam before its exhaustion is one possible measure of the antifoam durability.[8,20,25]

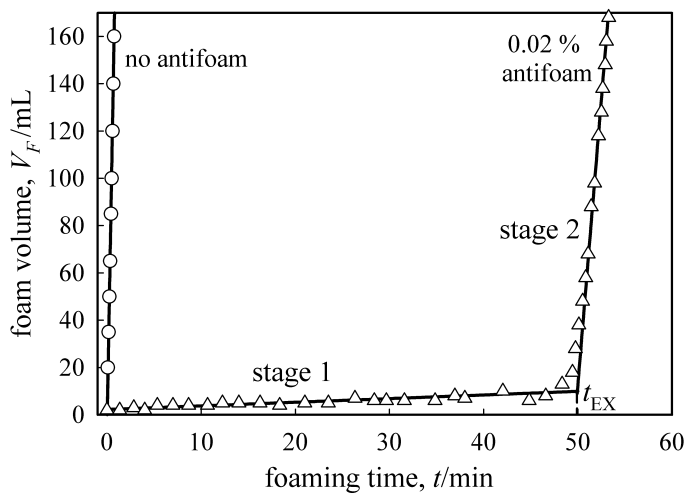

Figure 10.2. Foam volume V_F *versus* foaming time in the Foam Rise method (bubbling test) for a 10 mM AOT solution in the absence and in the presence of 0.02 wt. % silicone oil + silica particles compound (fast antifoam). Adapted from ref. 20.

1.2 Composition of antifoams and defoamers

A typical antifoam or defoamer consists of either oil droplets, hydrophobic solid particles or a mixture of both.[3-10] Various non-polar and polar oils (mineral and silicone oils, fatty alcohols, acids and esters, alkylamines and alkylamides, tributylphosphates, thioethers, nonionic surfactants above their cloud point)[3,8,9,29-31] are used as antifoam components. In cosmetic, personal care and some pharmaceutical products, the silicone oil polydimethylsiloxane (PDMS) has found wide application under the commercial name "dimethicone".[4] The solid particles are usually hydrophobized inorganic oxides (silica, Al_2O_3) or wax particles, *e.g.* Mg-stearate.[3-7] In

the process of froth flotation of ores and minerals, the role of foam destruction agents can be played by some of the processed particles and/or by the oily substances, introduced for enhancing the efficiency of the flotation process.

It was found empirically that mixtures of oil and hydrophobic solid particles (typically, 2-6 wt. % of particles dispersed in the oil phase) often have much higher antifoam efficiency, in comparison with each of the individual components.[3-8,23] Such antifoam compounds, if properly formulated, could prevent foam formation or destroy entirely the foam for seconds, at concentrations as low as 0.01 to 0.1 wt. % (see Figures 10.1 and 10.2). The mixture of PDMS and hydrophobized silica is a widely used antifoam compound in various technologies and consumer products (detergent powders, drugs) and it is sold under the commercial name "simethicone".[4] The reasons for the strong synergistic effect between oils and particles in the antifoam compounds are discussed in section 5 below.

The commercial antifoams are usually sold in the form of oil-in-water emulsions with mean drop size between 3 and 30 μm. The size of the solid particles in the antifoam compounds is typically between 0.1 and several μm. Observations by optical and electron microscopy show that the solid particles in oil-solid compounds tend to adsorb on the surface of the oil drops, see Figure 10.3.[3,8,19,28,32] Because these particles are too hydrophobic to create steric stabilization of the compound globules (similar to that occurring in Pickering emulsions), appropriate surface-active polymers or additional, more hydrophilic solid particles are used to stabilize the commercial compound-in-water emulsions. The comparative studies of foam destruction by compounds and their emulsions showed that virtually the same mechanisms are operative for both forms (note that the compound is actually emulsified in the surfactant solution during foaming).[8,10,12,19] That is why, in the following consideration, we do not differentiate between a compound and its emulsion.

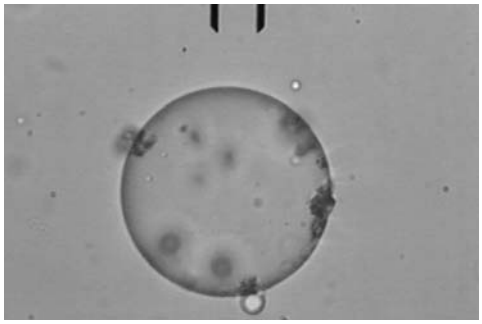

Figure 10.3. Optical microscopy image of antifoam globule containing silicone oil and silica particles (the dark objects of irregular shape adsorbed on the drop surface) dispersed in surfactant solution.

Scale bar = 32 μm. Adapted from ref. 8.

The terms antifoams and defoamers are usually used as synonyms. Sometimes, these terms distinguish two different ways of applying foam-destruction agents, which might have similar composition.[5,6] The antifoams are pre-dispersed in the foaming solutions with the major

aim to prevent the formation of excessive foam upon solution agitation. In contrast, defoamers are sprayed or spread over an already formed foam column, with the major aim to induce rapid foam collapse ("shock effect"). In this chapter we do not emphasize the differences between antifoams and defoamers, because the basic mechanisms of foam destruction are similar for both substances. The main difference between antifoams and defoamers from a mechanistic viewpoint is the importance of the so-called "entry barrier", which characterizes how difficult it is for a pre-dispersed antifoam globule to enter the air-water surface. Since the defoamers are applied from the air phase, there is no entry barrier to prevent their appearance on the foam surface. The latter circumstance facilitates foam destruction by a defoamer, even when the entry barrier for pre-dispersed antifoam of the same composition is relatively high and, hence, the antifoam is not very efficient. All results presented here are obtained with surfactant solutions typical of detergent and personal care products, with antifoams that were pre-dispersed in the solutions prior to starting the foaming process.

1.3 Aim and structure of the chapter

The major aim is to present briefly our current understanding of the basic mechanisms of foam destruction by various types of antifoam entities – solid particles, oil drops and globules of mixed oil-solid compounds. The antifoam mechanisms always involve attachment of these entities to the fluid air-water interface, often followed by bridging of the surfaces of two neighboring bubbles and subsequent bubble coalescence. As explained in section 5 below, the attachment of solid particles to the oil-water interface in antifoam compounds is very important for their high activity. Therefore, one could not explain the mechanisms of antifoaming without a detailed analysis of the particle-fluid interface interactions.

The paper is organized in the following way: First, the structural elements of a foam and the characteristic timescales of foam dynamics, in relation to the mechanisms of antifoam action, are discussed in section 2. Then, the mechanisms of foam destruction by solid particles are discussed in section 3, by oil drops in section 4 and by compound globules in section 5. Depending on the particular type of antifoam entities and on the specific mechanism of foam destruction, the main factors affecting the antifoam performance are discussed throughout these sections. The process of exhaustion of the antifoam compounds is discussed in section 5.3.

2 Foam structure, dynamic timescales and general modes of antifoam action

In this section we describe the general phenomena observed in the processes of foam formation and decay. The description is mostly phenomenological, without considering details of the specific mechanisms of antifoam action. These details depend strongly on the type of antifoam used (solid particles, oil drops or mixed oil-solid globules) and are discussed in the following sections 3 to 5.

2.1 Foam structure

The bubble compaction in foams leads to the formation of several structural elements which have different dimensions and play different roles in the processes of foam destruction by antifoams. These elements are[7,33,34] the foam films intervening between two adjacent bubbles, the Plateau Borders (PBs) and the nodes where four PBs meet with each other, see Figure 10.4. Since the characteristic dimensions and the capillary pressures of the PBs and their neighboring nodes are very similar, we discuss explicitly only the PBs, keeping in mind that the same phenomena (water drainage, oil drop entrapment and compression) occur in the nodes.

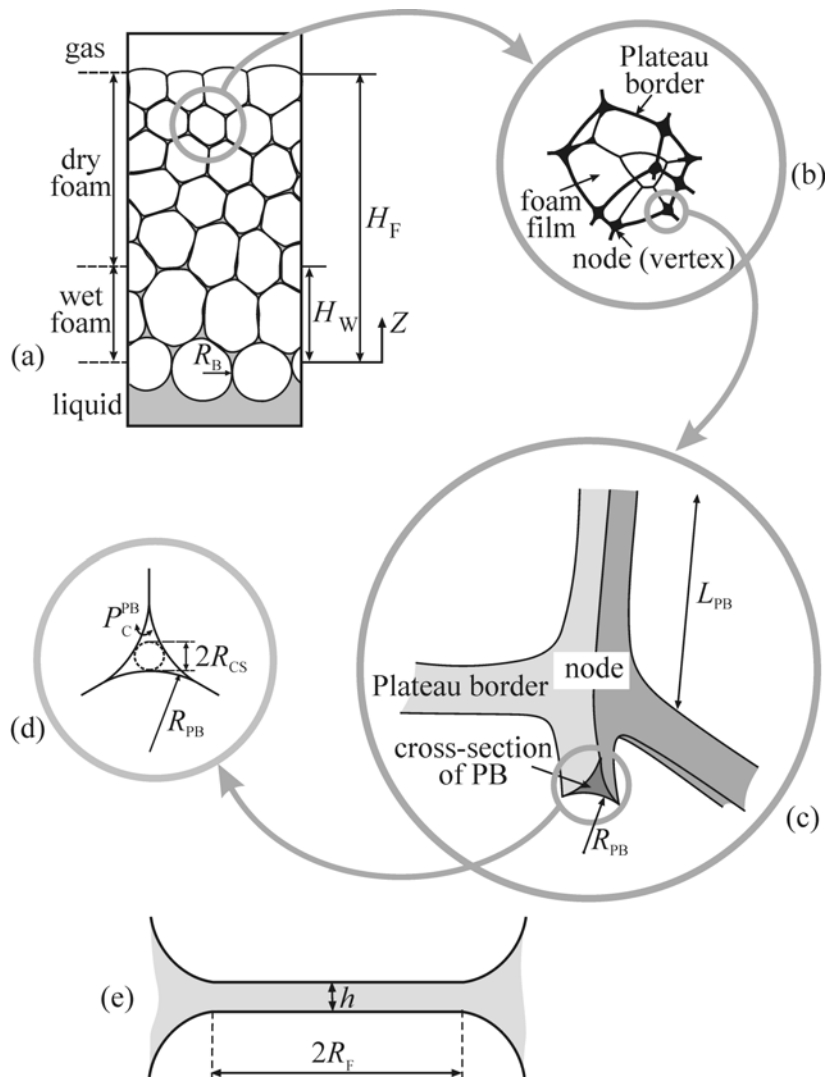

Figure 10.4 Schematic presentation of (a) foam column which is wet at the bottom and dry at the top and (b)-(e) the basic structural elements of the foam.

In the current section we discuss the characteristic dimensions of the foam films and PBs for foams, which are in mechanical equilibrium with underlying surfactant solution, under the

action of gravity. The dynamics of approaching this equilibrium and the characteristic timescales of the respective processes are considered in the following section 2.2.

2.1.1 Foam films

The foam films are characterized by their thickness, h, and radius, R_F, see Figure 10.4(e). The film radius in dry foams (with volume fraction of air $\phi_A > 98$ %) is about twice as small as the bubble radius, $R_F \approx 0.5R_B$. The equilibrium film thickness, h_{EQ}, is determined by the balance of the capillary pressure of the Plateau border walls, P_C^{PB}, and the disjoining pressure, $\Pi(h)$, which characterizes the forces acting between the two opposite surfaces of the foam film. The capillary pressure is defined as the difference between the pressure in the bubbles and the pressure in the liquid contained in the neighboring PBs, $P_C^{PB} = P_B - P_L$. At equilibrium, P_C^{PB}, which is the driving pressure for thinning of the foam films, is exactly counterbalanced by the repulsive disjoining pressure:[7,34-37]

$$\Pi\left(h_{EQ}\right) = P_C^{PB} \tag{10.1}$$

Equation 10.1 can be used to determine h_{EQ} if the functional dependence $\Pi(h)$ is known. Explicit expressions for the various components of the disjoining pressure can be found in the literature and are not reproduced here.[35-37]

The conventional components of the disjoining pressure (electrostatic, van der Waals, steric, oscillatory, etc.) are short ranged, so that h_{EQ} is typically smaller than 100 nm. Since the typical antifoam globules have larger diameter, $d_A > 1$ μm, the equilibrium foam films are too thin to contain such globules. An exception is worthwhile mentioning. If the foam films are stabilized by solid particles (which can sometimes be the case with foams encountered in pulp and paper production, drug manufacturing and foods), the equilibrium film thickness is determined primarily by the size of these particles and could be well above 100 nm.[38-40] In these cases, the equilibrium foam films could be sufficiently thick to contain antifoam globules. Note also that oils spread on the surfaces of the foam films could affect the film stability (by modifying, *e.g.*, the disjoining pressure Π), even when the films are very thin and do not contain any antifoam globules.[15]

2.1.2 Plateau borders

Two vertical regions are distinguished in equilibrium foam columns – a "wet" portion at the bottom of the foam column, with ϕ_A gradually increasing from ≈ 76 % up to ca. 98 %, and an upper layer of "dry foam" with $\phi_A > 98$ %, see Figure 10.4(a). In the wet portion of the foam, the hydrostatic pressure, $P_g = \rho g Z$, is comparable in magnitude to the capillary pressure of a single, non-compressed bubble (ρ is the mass density of the aqueous phase, g is the acceleration of gravity and Z is the vertical coordinate with origin placed at the bottom of the foam, see Figure 10.4). Hence, only slight to moderate deformation of the bubbles is sufficient to ensure

mechanical equilibrium here. The height of the wet portion of the foam, H_W, can be estimated by comparing the capillary pressure of a non-deformed bubble, $P_C^{NB} = 2\gamma_{aw}/R_B$ (where γ_{aw} is the air-water surface tension) with the hydrostatic pressure $P_g(H_W) = \rho g H_W$. This estimate leads to $H_W \sim 2\gamma_{aw}/(\rho g R_B)$, which is of the order of a centimeter for millimeter-sized bubbles. Therefore, foam columns with height above ca. several centimeters are prevailingly "dry" at equilibrium.

The bubbles in the upper, dry portion of the foam are strongly deformed to ensure sufficiently high capillary pressure, P_C^{PB}, which is able to compensate the increased hydrostatic pressure of the liquid in the PBs.[33,34] Important features of the dry foam are: (i) the main fraction of its liquid content is contained in the PBs and (ii) the length of the PBs, L_{PB}, is much larger than their cross-sectional dimension. For equilibrium dry foam, one can estimate the two characteristic dimensions of the PBs, namely the cross-sectional radius, R_{CS}, and the radius of curvature of the PB wall, R_{PB}, which play important roles in the process of antifoam globule entry. R_{CS} determines whether antifoam globules of given radius get trapped or move freely in the interconnected network of PBs and nodes, whereas R_{PB} determines the capillary pressure, P_C^{PB}, which compresses the trapped antifoam globules, see section 4.3.

To estimate R_{CS} and R_{PB} in the dry portion of the foam, one can start with the balance of the hydrostatic pressure, $P_g = \rho g Z$ (which is the driving force for water drainage from the foam column) and the capillary pressure, P_C^{PB} (which is the driving pressure for water suction from the surfactant solution into the foam):[7,8,14,16,34]

$$P_C^{PB}(Z) \approx \rho g Z \tag{10.2}$$

Then, the radius of curvature of the wall of the Plateau channel, R_{PB}, can be estimated from P_C^{PB} by the expression[7,8,16,34]

$$R_{PB}(Z) = \frac{\gamma_{aw}}{P_C^{PB}(Z)} = \frac{\gamma_{aw}}{\rho g Z} \tag{10.3}$$

Finally, the cross-sectional radius of the PB, R_{CS} (which is equal to the radius of a sphere inscribed in the Plateau channel, Figure 10.4(d)), can be found from geometrical considerations[8,14,16]

$$R_{CS}(Z) = \left(\frac{2\sqrt{3}}{3} - 1\right) R_{PB}(Z) \approx 0.155 \frac{\gamma_{aw}}{\rho g Z} \tag{10.4}$$

These estimates are used in section 4.3 to explain the effects of oil drops (as antifoams) and co-surfactants (as foam boosters) on foam stability.

2.2 Dynamics of foam evolution in the absence of antifoams

The foam evolution in the absence of antifoams is governed mainly by three inter-related processes: (i) thinning of the foam films, (ii) water drainage from the foam column and (iii) bubble coarsening due to gas diffusion from the smaller to the neighboring larger bubbles across

the intervening foam films (analogous to Ostwald ripening of small crystallites and emulsion droplets).[7,15,33] The fourth possible process, namely bubble coalescence as a result of foam film rupture, is not considered in this sub-section, because we are interested mainly in foams which do not decay in the absence of antifoams.

The aforementioned processes (i)-(iii) are characterized by different timescales, which have an important impact on the modes of foam destruction by various antifoams. For this reason, the characteristic times of these processes are briefly described below and used in the subsequent section 2.3 to explain the observed general modes of antifoam action.

2.2.1 Dynamics of foam film thinning

Optical observations of millimeter-sized foam films, formed from solutions of low molecular mass surfactants like those used in detergency, showed that film thinning typically occurs in several consecutive stages, see Figure 10.5.[6,7,14,36]

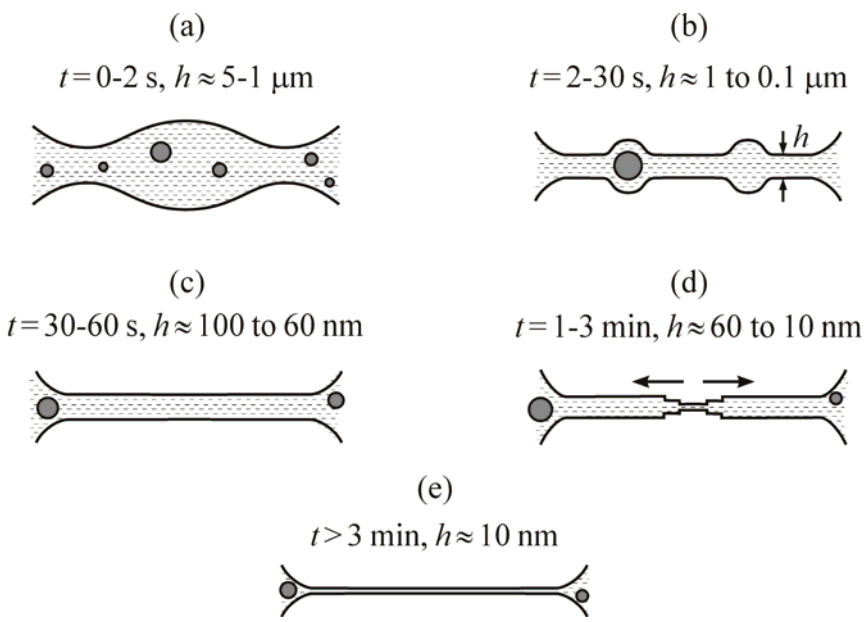

Figure 10.5. Main stages of foam film thinning: (a) Convex lens shaped "dimple", (b) planar film containing thicker channels, (c) plane-parallel film, (d) stratification - stepwise film thinning through formation and expansion of thinner spots and (e) thin film which is in equilibrium with the surrounding meniscus. The antifoam drops/particles are also shown schematically for comparison with the film thickness in the respective stage.

Dimple formation ($t \approx$ 0-2 s, $h \approx$ 5 to 1 μm) is where a convex-lens-shaped "dimple", with larger thickness in its center, is initially formed upon the mutual approach of two bubbles. This configuration is hydrodynamically unstable and an asymmetric outflow of liquid from the film leads to dimple disappearance within seconds after film formation. Drainage of a relatively thick planar film containing channels ($t \approx$ 2-30 s, $h \approx$ 1 to 0.1 μm) follows in which the film contains several channels (dynamic regions with thickness 200-500 nm larger than the remaining planar

portion of the film) and gradually thins down. Drainage of the thin plane-parallel film ($t \approx$ 30-60 s, $h \approx$ 100 to 60 nm) is the process in which the film has almost uniform thickness which gradually decreases with time. Film stratification ($t \approx$ 1-3 min., $h \approx$ 60 to 10 nm, see Figure 10.5(d)) is the stage realized in surfactant solutions with sufficiently high micelle volume fraction. The film thins in consecutive steps, which are due to oscillatory structural forces caused by "layering" of micelles in the film interior.[6,35,37,41,42] Each stepwise transition corresponds to a reduction of the number of micelle layers in the film (5 to 4, 4 to 3, *etc.*). Finally, the equilibrium black film (t > 3 min., $h \approx$ 5-10 nm) appears in equilibrium with the surrounding meniscus.

The experiments with larger, centimeter-sized foam films also showed an initial stage of dimple formation, followed by hydrodynamic instability, which led to liquid outflow and reduction of the film thickness down to 1-2 μm within several seconds after film formation.[10] An important conclusion from the observations of foam film dynamics is that the first stages of film thinning are very short and the film thickness becomes smaller than the diameter of the typical antifoam globules, d_A > 1 μm, in less than 30 seconds. This fact implies that the antifoam globules, which are trapped in the foam films in the initial stage of film formation, should either break the films in less than 30 seconds or should leave them with the draining water. Thus one can estimate the characteristic time of foam film thinning, in relation to film rupture by antifoam globules, as $\tau_F \sim 30$ s.

The rate of foam film thinning is sometimes estimated by the Reynolds equation (see *e.g.* ref. 43):

$$V_{RE} = -\frac{\mathrm{d}h}{\mathrm{d}t} = \frac{2}{3}\frac{h^3}{\eta R_F^2}\left[P_C - \Pi(h)\right] \tag{10.5}$$

where V_{RE} is the rate of film thinning, P_C is the capillary pressure of the bubble, $\Pi(h)$ is the disjoining pressure, R_F is the film radius and η is the fluid viscosity. For h larger than ca. 50 nm, $\Pi(h)$ is usually negligible in comparison with P_C, and the driving pressure for film thinning can be estimated as $P_C \sim 2\gamma_{aw}/R_B$, where $\gamma_{aw} \approx 30$ mN m^{-1} and R_B is the bubble radius. The comparison of the theoretical predictions of equation 10.5 with the optical observations of foam films showed that Reynolds equation strongly under-estimates the rate of foam film thinning (*i.e.* the characteristic time of film thinning is strongly over-estimated), especially for foam films with diameter of the order of centimeters or millimeters. Theoretical and experimental studies showed[43-46] that this large discrepancy is due to the fact that the foam film surfaces in systems stabilized by low molecular mass surfactants are not usually plane-parallel or tangentially mobile. These two effects are not accounted for in the Reynolds equation and lead to faster film thinning, in comparison with the prediction of equation 10.5. Therefore, the Reynolds equation is rarely appropriate for estimating the rate of thinning of foam films with diameter above 1 mm, in relation to the antifoam effect.

2.2.2 Water drainage from quiescent foams

Recent theoretical and experimental studies[47-51] revealed three main periods in the water drainage from foam columns. The characteristic time, τ_{DR}, of the first two periods, which are governed by gravity, could be estimated by considering the water flow through the network of PBs and nodes. This network is considered as a porous medium with certain permeability, which depends on the liquid volume fraction, ϕ_L, and changes in the course of the drainage process.[47,49] The following estimate was derived theoretically[49] and confirmed experimentally for τ_{DR}

$$\tau_{DR} \sim \frac{H_F}{v_F} = \frac{H_F}{\left(K_m \rho g R_B^2 / \eta\right)\phi_L^m} \qquad m = ½ \text{ or } 1 \tag{10.6}$$

where H_F is the foam height, v_F is the average velocity of the liquid through the network of PBs, K_m is a numerical constant ($K_1 \approx 6\times10^{-3}$ and $K_{1/2} \approx 2\times10^{-3}$) and m is a parameter which takes the value of 1 or ½ for tangentially immobile and tangentially mobile surfaces of the PBs, respectively. For the effects of tangential mobility, see refs. 49 and 50. Taking a typical value for a wet foam with $\phi_L \approx 0.25$, generated from an aqueous surfactant solution with $\rho = 1000$ kg m^{-3}, one obtains the following estimate for the characteristic time of water drainage from the foam

$$\tau_{DR} \sim \frac{H_F \eta}{10 R_B^2} \tag{10.7}$$

Thus, for a foam with height $H_F = 20$ cm and mean bubble diameter $2R_B = 1$ mm, made from aqueous solutions with viscosity $\eta = 1$ mPa s, one obtains $\tau_{DR} \approx 80$ s. As seen from equation 10.7, the characteristic drainage time strongly depends on bubble size and solution viscosity. The decrease of bubble diameter by a factor of 3 (down to 300 μm) leads to an increase of τ_{DR} up to 750 s.

The theoretical models[47,49] predict that the first stage of water drainage lasts for a period $\tau_{DR}/(m+1)$, and during this stage about half of the total liquid contained in the initial foam, V_{L0}, drains linearly with time

$$V_{DR}(t)/V_{L0} = \frac{t}{\tau_{DR}} \qquad t \le \tau_{DR}/(m+1) \tag{10.8}$$

The drainage of the remaining fraction of liquid during the second stage is somewhat slower and proceeds according to the expression:

$$V_{DR}(t)/V_{L0} = 1 - \frac{m}{(1+m)^{1+1/m}}\left(\frac{\tau_{DR}}{t}\right)^{1/m} \qquad t \ge \tau_{DR}/(m+1) \tag{10.9}$$

The latter equation shows that 95 % of the liquid drains for 2 to 4 times τ_{DR}, depending on the tangential mobility of the PB walls, *i.e.* on the value of $m = 1$ or 1/2. As an illustration, Figure 10.6 presents the theoretically calculated volume of the liquid remaining in the foam during the process of water drainage, $V_L(t)/V_{L0} = [V_{L0} - V_{DR}(t)]/V_{L0}$, in accordance with equations 10.8 and

10.9. Note that water drainage can be slower in the presence of solid particles or oil drops in the foam, because these particles/drops obstruct the PBs and nodes, thus increasing the hydrodynamic resi ıtions 10.6-9.[5,6,14]

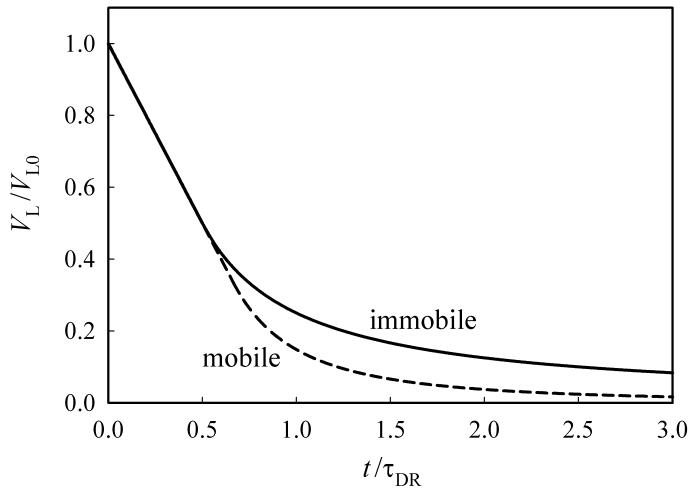

Figure 10.6. Change of the normalized liquid volume in the foam V_L/V_{L0} with the dimensionless time t/τ_{DR} as a result of water drainage. The theoretical predictions for bubbles with tangentially immobile (solid curve) or mobile (dashed curve) surfaces are plotted in accordance with equations 10.8 and 10.9.

The theoretical modeling predicts that there is a third, much slower stage of liquid drainage, characterized by an exponential approach to the final equilibrium configuration of the foam at which the gravity force is counter-balanced by the capillary suction of the PBs.[48]

2.2.3 Characteristic time of bubble coarsening due to gas diffusion

Another process, which strongly affects the foam evolution, is the bubble coarsening due to gas diffusion across the foam films, from the smaller to the larger bubbles. The respective increase of the mean bubble radius is described by the expression[52,53]

$$R_B = R_{B0}\left(1 + t/\tau_{CR}\right)^{1/2} \tag{10.10}$$

where R_{B0} is the initial mean bubble radius. The characteristic time of bubble coarsening, τ_{CR}, can be estimated from the expression[53]

$$\tau_{CR} = R_{B0}^2 / \left[2D_{EFF}\alpha\left(\phi_L\right)\right] \tag{10.11}$$

where D_{EFF} is an effective diffusion coefficient of the gas transport across the foam films, which depends on the material properties of the gas and the solution. The function $\alpha(\phi_L)$ accounts for the dependence of the radius of the foam films on the liquid volume fraction in the foam and is described by the semi-empirical expression[53]

$$\alpha\left(\phi_L\right) = \left[1 - 1.5\phi_L^{1/2}\right]^2 \tag{10.12}$$

For dry foams containing air bubbles, $D_{EFF} \sim 5\times10^{-10}$ m^2 s^{-1} and $\alpha(\phi_L) \approx 1$, which allows one to estimate $\tau_{CR} \approx 250$ s for bubbles with initial diameter $2R_{B0} = 1$ mm, and $\tau_{CR} \approx 30$ s for bubbles with $2R_{B0} = 300$ μm. Note that bubble coarsening decelerates with time, because the mean bubble size gradually increases.

2.2.4 Comparison of characteristic times for film thinning, water drainage and bubble coarsening

The comparison of the characteristic times of foam film thinning, τ_F, water drainage from the foam, τ_{DR}, and bubble coarsening, τ_{CR}, indicates that τ_F is usually shorter than both τ_{DR} and τ_{CR}. In other words, the foam films thin relatively rapidly, whereas the water drainage and bubble coarsening from the foam require longer time. For a typical foam with mean bubble diameter $2R_B = 1$ mm, one estimates $\tau_{DR} < \tau_{CR}$, *i.e.* drainage dominates the initial stage of foam evolution, as compared to bubble coarsening. In contrast, for foams containing smaller bubbles with $R_B <$ 400 μm, τ_{CR} is shorter than τ_{DR} (*i.e.* the coarsening will be faster than drainage in the initial stage of foam evolution), due to the opposite dependences of τ_{DR} and τ_{CR} on R_B, see equations 10.7 and 10.11. At long times, $t >> \tau_{DR}$, the processes of water drainage and bubble coarsening couple with each other and proceed in parallel.[51,53] The coarsening leads to a gradual increase of the mean bubble size, which is inevitably accompanied with a decrease of the number density of PBs and nodes per unit volume of the foam, and a slow drainage of the formed excess water.

Let us recall that the equilibrium PB cross-section, $R_{CS} \sim 5$ to 50 μm, is about two to three orders of magnitude larger than the equilibrium film thickness, $h_{EQ} < 50$ nm. The different magnitudes of R_{CS} and h, and the different timescales of the various processes, have important implications for the modes of antifoam action, which are discussed in the following sub-section.

2.3 Dynamics of foam destruction by antifoams

2.3.1 Location of the antifoam globule entry - fast and slow antifoams

The fact that the foam films become rapidly thinner than the antifoam globule size, whereas the PBs remain larger than these globules for longer time, means that there are two different scenarios for foam destruction by antifoams.[3,6,8,13] Foam film rupture by antifoam globules in the early stages of film thinning includes the formation of a particle bridge (for solid particles) or an oil bridge (for oil drops or mixed oil-solid compounds) between the two opposite surfaces of the foam film - see sections 3.1 and 4.1 below. If the formed bridge is unstable, it ruptures the foam film within seconds after its formation, see Figure 10.7. As a result, this mechanism of foam film rupture usually leads to complete foam destruction in a short period of time (seconds to tens of seconds); see the results for the oil-silica compound in Figure 10.1 for example. The term "fast antifoam" is used to denote substances which destroy the foam by this film-breaking mechanism.[8] The experiments showed[8,10-13,19-23] that mixed globules of appropriately formulated

oil-solid compounds often (though not always) behave as fast antifoams, in which the solid particles ensure an ultra-low entry barrier, whereas the oil (if appropriately chosen) ensures unstable oil bridges.

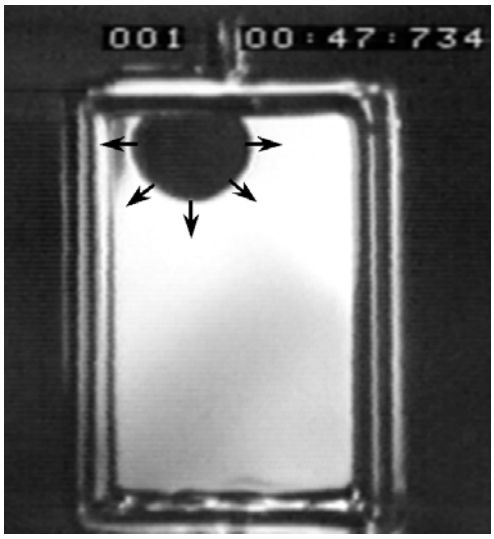

Figure 10.7. Image of a large (2 × 3 cm) foam film from a 10 mM AOT solution containing 0.01 wt. % of silicone oil + silica particles emulsion (fast antifoam) taken about 1 second after the film was formed and several milliseconds after appearance of a hole in the film. The hole expands (illustrated by the black arrows) and eventually leads to film rupture. The observations are made by high-speed video camera. Taken from ref. 11.

By contrast, foam cell destruction after antifoam globule entry in the PBs and nodes can also take place. Here, the antifoam globules which are unable to break the foam films in the early stages of film thinning are first accumulated in the adjacent PBs. They are afterwards compressed by the walls of the shrinking PBs (as a result of water drainage from the foam) and eventually enter the walls of the PBs, causing rupture of the neighboring foam films.[5,6,8,54] The foam destruction by this mechanism usually requires minutes or tens of minutes, because the water drainage from the foam (needed for compression of the trapped drops) is a slow process; see the results for silicone oil in Figure 10.1 for example. Furthermore, one usually observes residual foam which may remain stable for hours (the respective explanation is described in section 4.3). The term "slow antifoam" is used to describe substances which destroy the foam by this mechanism.[8] The oil drops deprived of solid particles usually behave as slow antifoams.[5,6,8,14-18]

As explained in section 4.3, one of the main factors determining whether a given antifoam would behave as fast or slow is the magnitude of the entry barrier of the antifoam globules. If the repulsive forces acting between the antifoam globules and the surfaces of the foam film are too strong, *i.e.* the entry barrier is high, the globules leave the foam film without forming bridges and the respective antifoam behaves as slow.

2.3.2 Effect of antifoams on foaming – role of the kinetics of surfactant adsorption

In general, the fast antifoams strongly reduce the foaminess of surfactant solutions, whereas the slow antifoams affect the foaminess only slightly.[8,14,15,17] To explain these effects, let us consider the process of foaming by agitation, *viz.* by shaking, stirring or pouring the solution from a nozzle. Such agitation leads to entrapment of air into the solution and to the formation of a wet foam with an air volume fraction below ca. 80 %, in which the bubbles collide with each other. Foam films with thickness of several micrometers are formed in the zone of bubble-bubble contact. However, the intensive agitation rapidly separates the colliding bubbles from each other, so that the foam films have no time to thin. The film thickness remains larger than ca. 1 μm during the entire duration of the bubble encounters.

Therefore, an antifoam could reduce the solution foaminess only if its globules are able to destroy relatively thick foam films, that is, if the antifoam behaves as fast. It is rather common to observe a weak effect, or even an increased foaminess of the surfactant solutions in the presence of dispersed oil droplets, whereas the same droplets may have a noticeable (slow) antifoam effect in quiescent foams generated from the same solutions (*e.g.* the results for silicone oil in Figure 10.1). The increased foaminess observed sometimes in the presence of oil-based antifoams is explained by reduced surface tension (as a result of oil spreading on the solution surface), which facilitates the expansion of the air-water surface and air entrapment.[17]

One particular feature of the antifoam effect during foaming and upon foam shear (*i.e.* under dynamic conditions) is that the antifoam activity can be affected strongly by the kinetics of surfactant adsorption.[8,19,32,55] The reason is that the bubble generation and deformation are related to the creation of new air-water surface, and it takes a certain time to cover this surface with a protective adsorption layer of surfactant. The kinetics of surfactant adsorption is particularly important for solutions of nonionic surfactants, because the de-micellization rate and the monomer concentration are rather low in such solutions. As a result, the respective characteristic time of surfactant adsorption is often of the order of seconds and tens of seconds, which results in the formation of under-saturated adsorption layers upon bubble-bubble collision in dynamic foams. This effect facilitates the entry of the antifoam globules at the foam film surfaces and the subsequent foam film rupture in agitated foam, whereas the same antifoam could be rather inactive in quiescent foam of the same composition.

As an illustration of the effect of surfactant adsorption rate on the antifoam activity, we compare the foaminess and the foam stability of 10 mM AOT (anionic) and 0.6 mM APG (alkyl polyglucoside, nonionic) solutions (approx. 4 × critical micelle concentration, CMC) in the absence and in the presence of 0.01 wt. % silicone oil-silica compound. As seen from Figure 10.8(a), the initial foam volume generated by shaking AOT solutions in the presence of antifoam is several times larger than that generated from APG solutions under equivalent foaming conditions. However, after stopping the agitation, the AOT foam completely disappears within seconds, whereas the APG foam remains stable for hours. The reference samples of AOT and

APG solutions (without antifoam) show rather good foaminess and no foam destruction in the timescale of Figure 10.8(a).

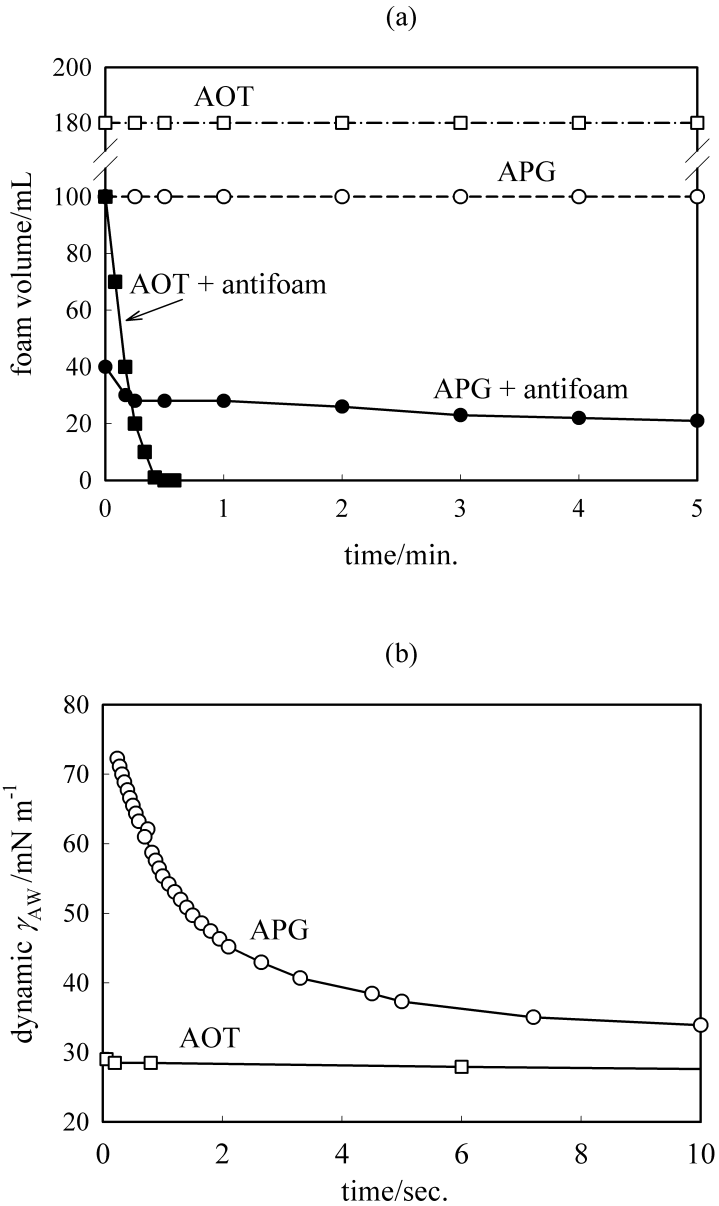

Figure 10.8. (a) Foam volume versus time for two surfactant solutions, 10 mM AOT and 0.6 mM APG, in the presence and in the absence of 0.01 wt. % silicone oil + silica compound (Bartsch test). (b) Dynamic surface tension of the same solutions measured by the maximum bubble pressure method in the absence of antifoam. Adapted from ref. 19.

The results from related model experiments allowed us to explain the observed differences of the antifoam performance in AOT and APG solutions.[19] Measurements of the dynamic surface tension showed a very large difference in the adsorption kinetics of the two surfactants; more than 10 seconds were needed for saturation of the adsorption layer in the APG solution, whereas this process took less than 0.1 seconds in the AOT solution, see Figure 10.8(b). Further, the entry barrier of the compound globules was much lower in AOT solutions (≈ 3 Pa)

compared with APG solutions (> 125 Pa) for saturated adsorption layers. The ultra-low entry barrier in AOT solutions explains why the antifoam globules are able to rapidly rupture the foam films in both agitated and quiescent AOT foams, whereas the high entry barrier in APG solutions precludes the foam film rupture in the APG-stabilized quiescent foams. Hence, the studied antifoam had significant activity in the foaming APG solution, mainly due to the slow APG adsorption. If the kinetics of APG adsorption was as fast as that of AOT, the antifoam would be much less efficient in suppressing the foaminess of APG solutions.

It is worthwhile noting that the results for APG-stabilized foams in Figure 10.8(a) illustrate the possible switch of a given antifoam from fast (during foaming) into slow (in the quiescent foam). Indeed, the foaminess of the APG solution was strongly reduced in the presence of antifoam compound, whereas the evolution pattern of the quiescent APG foam was indicative of the action of a slow antifoam. As explained in the previous paragraph, such pattern reflects a low entry barrier of the antifoam globules during foaming due to formation of incomplete adsorption layers, and a high entry barrier when the adsorption layers are completed. Hence the antifoam behaves as fast (film breaking) during foaming and transforms into slow (acting through entry in the PBs) when the agitation is stopped and the surfactant is allowed to form complete adsorption layers on the foam film surfaces.

2.3.3 Effect of antifoams on the evolution of static (quiescent) foams

As already explained, the fast antifoams are able to destroy completely quiescent foams in a very short period of time (typically 3 to 30 s, depending on the antifoam activity and concentration), by rupturing the foam films in the early stages of their thinning. This means that the only important characteristic dimension in the foam is the film thickness, h, as compared to the diameter of the antifoam globules, d_A, and the relevant timescale is τ_F, which is imposed by the process of film thinning down to a thickness $h \sim d_A$. The other timescales discussed in section 2.2 are too long to play important role in the process of foam destruction.

In contrast, the dynamics of foam destruction by slow antifoams, *e.g.* oil drops in surfactant solutions of high concentration, is related to the rates of water drainage and bubble coarsening, because drop entrapment and compression in the PBs is needed for accomplishing the antifoam globule entry and foam cell destruction. In general, four distinct stages are observed in the evolution of quiescent foams destroyed by slow antifoams, see Figure 10.9:[8,14,15]

(i) During period I, lasting for 1 to several minutes, the upper boundary of the foam does not change because no coalescence of the bubbles with the uppermost air phase takes place. The lower boundary of the foam rises with time, due to water drainage from the initially formed wet foam. During this stage the foam films rapidly thin down, the Plateau borders (PBs) and the nodes become much narrower (the duration of this stage is comparable to τ_{DR}) and the smallest bubbles shrink and disappear due to air diffusion across the foam films (characteristic time τ_C), *cf.* Figures 10.10(a) and (b).

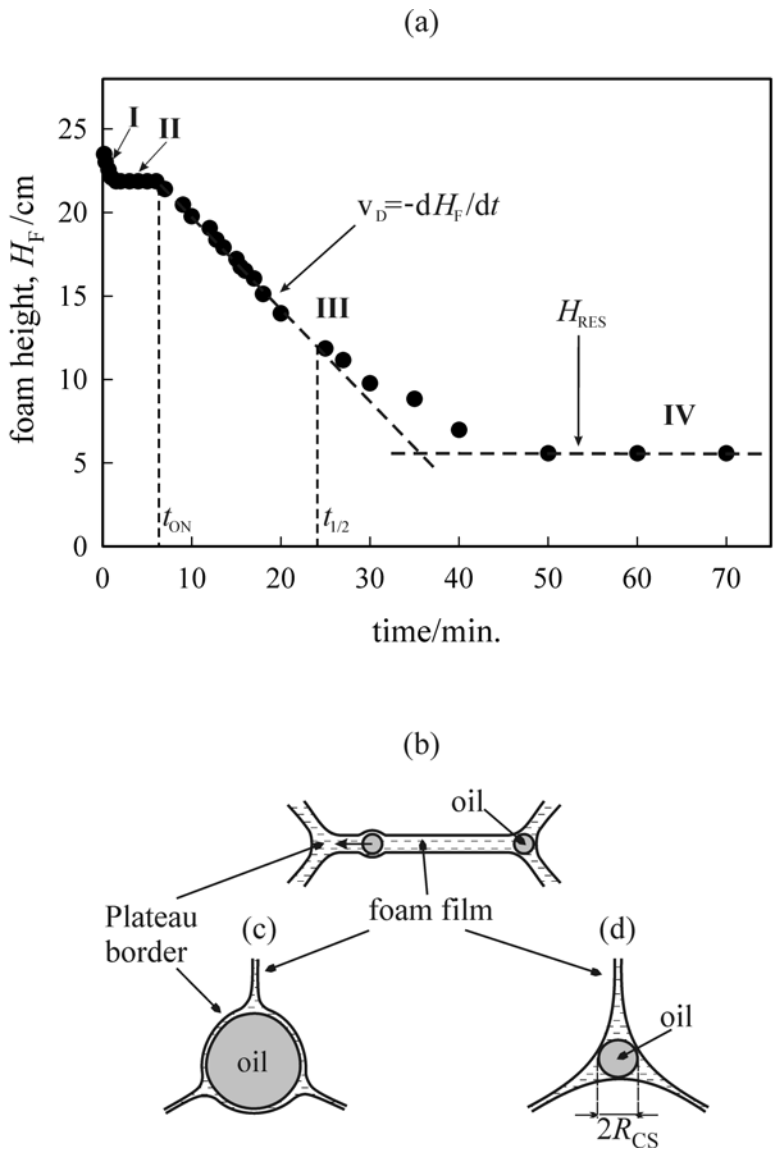

Figure 10.9. (a) Foam height, $H_F(t)$, *versus* time for a solution containing 0.1 M SDP3S (anionic surfactant), nonionic co-surfactant (foam booster) and 0.1 wt. % silicone oil as a slow antifoam. The time t_{ON} gives the onset of foam decay by bubble collapse and $t_{1/2}$ indicates the foam half-life. The roman numbers I-IV indicate different stages of foam evolution. Adapted from ref. 15. (b) Schematic presentation of the oil drop migration from the foam film into the adjacent Plateau border in the process of film thinning. (c) The walls of the shrinking Plateau border compress the oil drop and asymmetric oil-water-air films are formed. (d) If the drop diameter is smaller than the cross-section of the Plateau border, the drop is not compressed.

(ii) During stage II ($t >> \tau_{DR}$), the foam volume remains virtually constant because the water drainage is already very slow and no bubble coalescence occurs. However, optical observations evidence a significant restructuring of the foam cells during this period, due to bubble coarsening through air diffusion across the films. The latter process leads to a gradual, but significant decrease of the number density of PBs and nodes per unit volume of the foam. As a result, the antifoam globules gradually accumulate in the remaining nodes and PBs with time,

see Figure 10.10(c) and (d). In addition, the PBs and nodes slowly shrink with time due to water drainage from the foam, which leads to a decrease of the radius of curvature of the PB walls, R_{PB}, and to a gradual increase of the capillary pressure, P_C^{PB}, exerted by these walls on the trapped oil drops.

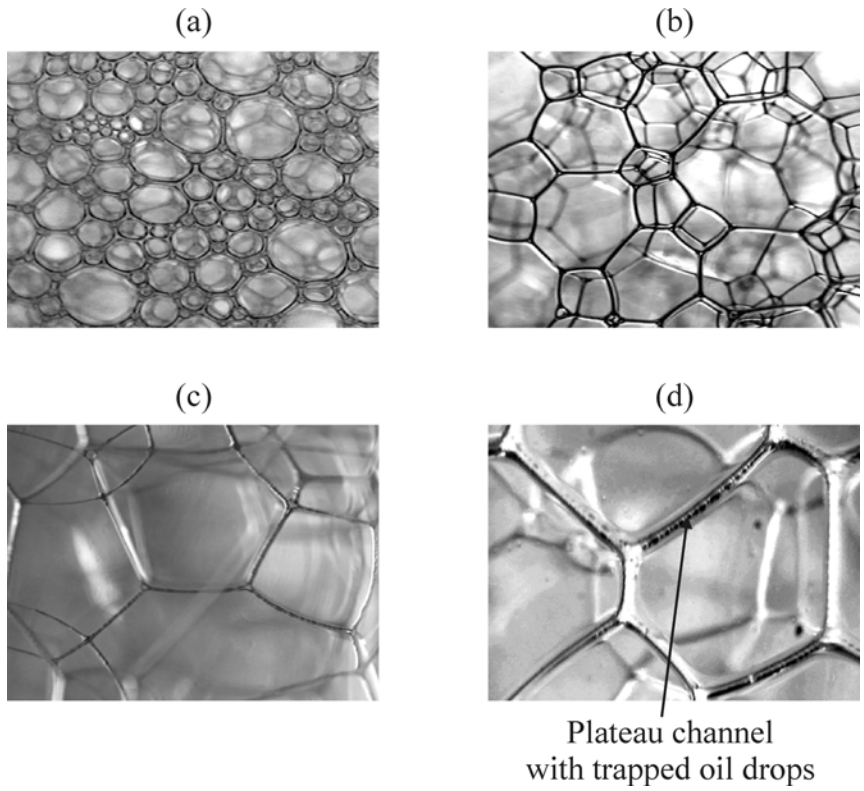

Figure 10.10. Photographs of foam cells just below the top of a foam column at different stages of the foam evolution, *cf*. Figure 10.9. (a) Wet foam in stage I. (b) Foam at the transition between stages I and II. (c) Air diffusion from the small bubbles towards the larger ones leads to the disappearance of the smallest bubbles and to the gradual accumulation of oil drops in the Plateau borders during period II. When the capillary pressure at the top of the foam column exceeds the entry barrier of the oil drops, a destruction of the uppermost layers of bubbles is observed which is the beginning of stage III (not shown). (d) Enlarged view of Plateau channel in which trapped oil drops are seen. Taken from ref. 15. The image size is 2×1.5 cm in (a)-(c) and 1×0.75 cm in (d).

(iii) When a certain critical value of P_C^{PB} is reached, the foam destruction starts, primarily through rupture of the upper layer of bubbles where the compressing capillary pressure is the highest. This is the onset of stage III, denoted by t_{ON} in Figure 10.9(a). The rate of foam destruction, $v_D = -dH_F/dt$, is approximately constant during the main course of period III (see also the results for silicone oil in Figure 10.1).

(iv) After a certain amount of foam is destroyed, the rate of foam decay gradually decreases and, eventually, stage IV is reached in which the foam volume remains almost constant for many minutes or even hours. Only large bubbles remain in the foam and the process of bubble coarsening is rather slow. The height of this residual, long-standing foam is denoted hereafter by H_{RES}. In section 4.3 below, the process of foam destruction by slow antifoams is

analyzed quantitatively, by relating the size of the antifoam globules and their entry barrier to the value of H_{RES} and to the stages of foam evolution described above.

3 Solid particles as antifoam entities

3.1 Bridging-dewetting mechanism of foam film rupture – characteristic timescales

Experimental and theoretical studies showed that solid particles could rupture foam films by the so called "bridging-dewetting" mechanism.[3,55-63] This mechanism implies that, first, the solid particle comes into contact with the two opposite surfaces of the foam film, forming a "solid bridge" between them, see Figure 10.11.

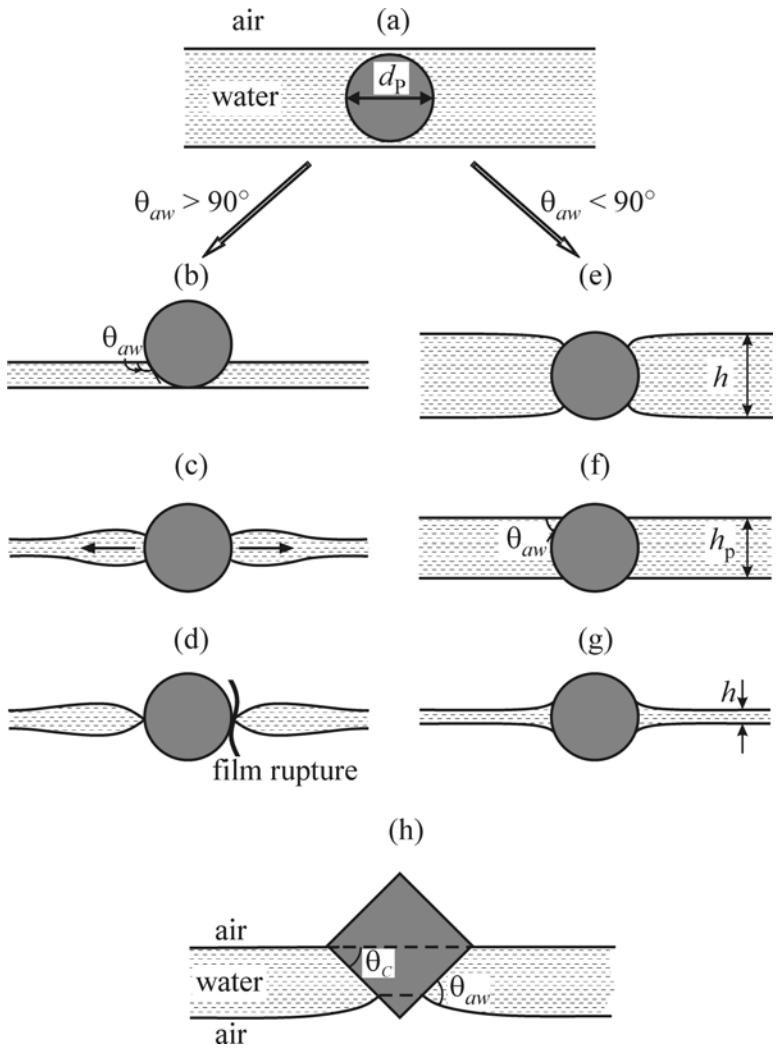

Figure 10.11. Schematic presentation of the bridging of foam film surfaces by a solid particle. (a)-(d) When the spherical particle has contact angle $\theta_{aw} > 90°$, it is dewetted by the liquid and the three-phase contact lines come into direct contact with each other perforating the foam film at the particle surface. (e)-(g) If the contact angle $\theta_{aw} < 90°$, the particle is not dewetted and the foam film remains stable. (h) Cone-shaped particle with slope angle θ_C can be dewetted if $\theta_{aw} > \theta_C$, when the particle is properly oriented to the film surfaces.

Second, if the particle is sufficiently hydrophobic, the liquid dewets the particle surface so that the three-phase contact lines eventually come into direct contact with each other; the foam film gets perforated at the particle surface, see Figure 10.11(a)-(d). The antifoam activity of solid particles is strongly related to their hydrophobicity, which is quantified by the three-phase contact angle air-water-solid, θ_{aw}, measured into water. Note that θ_{aw} depends not only on the particles used, but on the foaming solution as well.

Two timescales are important for the bridging-dewetting mechanism of foam film rupture by solid particles. First, the foam film should thin down to a thickness comparable with the particle diameter, d_P. This process is relatively fast, with a characteristic time $\tau_F(d_P) \leq 30$ s, unless d_P is smaller than ca. 1 μm. Therefore, if the particles are with diameter $d_P > 1$ μm, the rate of film thinning is not an obstacle for rapid foam destruction by this mechanism.

Another timescale is set by the moving contact lines along the particle surface, which push liquid from the vicinity of the particle into the neighboring film region, see Figure 10.11(c). The characteristic time of this process can be estimated as, $\tau_{DEW} \sim d_P/V_{DEW}$, where V_{DEW} is the sliding velocity of the contact lines along the particle surface. Direct optical observations by Dippenaar[58] showed that the motion of the contact lines (the particle dewetting) is very fast, $V_{DEW} \sim 1$ μm ms^{-1}. Theoretical estimates, based on the hydrodynamic theory of contact line motion,[43] predict similar value of V_{DEW}. By developing a detailed model of the dynamics of particle dewetting in foam films, Frye and Berg[55] calculated numerically τ_{DEW} and showed that, if the contact angle θ_{aw} is several degrees larger than the critical angle for dewetting (discussed in the next sub-section), τ_{DEW} is shorter than *ca*. 10 ms.

The above estimates show that the bridging-dewetting mechanism would lead to rapid foam destruction if solid particles with appropriate properties (see below) were present in the foaming solution. It is worthwhile noting that in detergency and many other applications where "strong" surfactants are typically used (*i.e.* very active surfactants with concentration above the CMC), solid particles are not very efficient foam breakers; the surfactant molecules adsorb on particle surfaces rendering them too hydrophilic to have a pronounced antifoam effect.[60-62] In such systems, oil-based antifoams are more efficient and have found wide application in practice.[3-5,60] On the other hand, foam control in the presence of solid particles is very important for the successful processing of ores and other minerals by the method of froth flotation, in which "mild" surfactants are typically used.

3.2 Influence of particle properties on antifoam effect

The two stages of the bridging-dewetting mechanism of foam film rupture by solid particles, Figure 10.11, imply two groups of important factors related to (i) bridge formation and (ii) particle dewetting. These factors are briefly discussed below.

With respect to bridge formation, the most important factors are the particle size and several other factors related to the particle entry barrier such as particle shape, surface charge, *etc*. As explained above, the particle size is not a problem for rapid bridge formation, unless $d_P <$

1 μm. The factors related to the entry barrier are more difficult to quantify. As shown by Kulkarni *et al.*,[64,65] the surface charge could create significant electrostatic repulsion between the particle and the surfaces of the foam films (*e.g.* in the presence of adsorbed ionic surfactant), which might result in high entry barriers. An indirect proof for the importance of this effect was recently found in studies of Pickering emulsions stabilized by spherical solid particles of micrometer size.[66] Emulsification experiments showed that the particles enter the oil-water interface and stabilize the emulsions easier if the electrostatic repulsion between the particle and the oil-water interface is suppressed (*e.g.* at high NaCl concentration in the aqueous phase). Otherwise, the electrostatic barrier hampers particle adsorption and no stable emulsions are formed. Other types of surface forces caused by surfactant micelles (oscillatory surface forces[35,41,42]), adsorbed polymer molecules (steric repulsion) *etc.*, could create significant entry barriers, which should be suppressed to effect bridge formation.

The experiments show that the entry barrier is strongly reduced and the bridges are easily formed when the particles have sharp edges. To explain this effect one can use Derjaguin's approximation,[67] which relates the force between a spherical particle and a planar surface, F_{PS}, with the disjoining pressure $\Pi_{PS}(H)$ between two planar surfaces, one of them being the foam film surface and the other (hypothetical) surface has the same properties as the particle surface:

$$F_{PS}(\delta) = 2\pi R_P \int_{\delta}^{\infty} \Pi_{PS}(H)\, dH \tag{10.13}$$

Here R_P is the particle radius, δ is the distance between the particle forehead and the planar surface and H is a running variable. As seen from equation 10.13, the interaction force is proportional to the particle radius and is therefore lower in magnitude for smaller particles. If the solid particle is non-spherical, equation 10.13 can be used with R_P being replaced by the radius of curvature of the particle forehead, which is very small for sharp edges. Hence, the entry barrier of a solid particle with sharp edges (if properly oriented) would be much smaller, as compared to the barrier of a spherical particle having the same overall dimension. This "pin effect" of the sharp edges strongly facilitates bridge formation for non-spherical particles.

With respect to dewetting, the most important factors are the particle hydrophobicity and shape. Theoretical and experimental studies[3,55,57-62] showed that the critical contact angle is 90° for complete dewetting of solid particles which have smooth convex surfaces, such as spheres, ellipsoids, disks and rods. Particles of contact angle $\theta_{aw} > 90°$ induce foam film rupture and foam collapse, see Figure 10.11(a)-(d). Less hydrophobic smooth particles ($\theta_{aw} < 90°$) do not cause film rupture; they can even stabilize the foam by blocking the Plateau channels and reducing the rate of water drainage from the foam, see Figure 10.11(a), (e), (f) and (g).

Various studies showed that foam films can be ruptured by less hydrophobic particles (θ_{aw} well below 90°) if the latter have sharp edges and are properly oriented in the film.[3,55,57,58] An illustrative example of this possibility is the theoretical prediction for a cone-shaped particle, whose axis is oriented perpendicularly to the film surface, Figure 10.11(h). Simple geometrical considerations show that cone-shaped particles with slope angle θ_C can be dewetted if

$$\theta_{aw} > \theta_C \tag{10.14}$$

Similar considerations imply that cubic particles with $\theta_{aw} > 45°$ could rupture foam films, if the particles are oriented with their diagonal being perpendicular to the film plane. Indeed, Dippenaar[58] showed experimentally that cubic galena particles with contact angle $\theta_{aw} \approx 80°$ rupture the foam films if the particles are properly oriented. Frye and Berg[55,63] and Garrett[57] showed that hydrophobic glass particles and poly(tetrafluorethylene) particles with irregular shape have a significant antifoam effect even when the contact angle $\theta_{aw} \approx 40°$. The *in-situ* formation of similar, sharp-edged soap precipitates is the most probable reason for the observed significant antifoam effect of calcium soaps in the recent study by Zhang *et al.*[68]

It is worthwhile noting that, if the particle is too hydrophilic to be dewetted by the liquid, the two contact lines on the particle surface acquire equilibrium positions which depend on the contact angle θ_{aw}, see Figure 10.11(f). The distance between the two equilibrium contact lines can be estimated for spherical particles by the expression

$$h_p = 2R_p \cos\theta_{aw} \tag{10.15}$$

Once such a stable bridge is formed, the evolution of the system depends on the ratio of the average film thickness, $h(t)$, and the value of h_p. Until $h(t) > h_p$, the particle remains in the foam film and causes local film thinning. When the average film thickness, h, becomes smaller than h_p, the particle is expelled from the film into the neighboring meniscus regions, which have local thickness equal to h_p. The reason for this migration of the particle outside the film is that the surface energy of the system (film + particle + meniscus) is minimal when the particle does not deform the film surfaces, so that no extra surface energy is created by the particle presence. In foams, such insufficiently hydrophobic particles can obstruct the Plateau borders and stabilize the foam as a result of the reduced rate of water drainage. Moreover, if the particles are of sufficiently high concentration to cover the entire bubble surface, the robust shell formed resists bubble shrinking and could arrest almost completely Ostwald ripening.

More detailed analysis of the role of shape, size and contact angle of solid particles for their antifoam activity can be found in the papers by Garrett,[3,57] Frye and Berg[55,63] and Aveyard *et al.*[59-62]

4 Antifoam effect of oil drops

The possible mechanisms of foam destruction by oil drops compared to solid particles are more versatile, due to the possibilities for oil bridge deformation and oil spreading. Several scenarios of foam destruction by oils were proposed in the literature and are discussed in this section.

In most cases, the oil drops destroy the foams through an initial accumulation in the Plateau borders and nodes, *i.e.* the drops behave as slow antifoams.[5-8,14-18,54] This is due to the relatively high entry barrier when the drops are dispersed in surfactant solutions typical for detergency. The oil drops are able to act as fast antifoams and to break the foam films by the bridging mechanisms, described in section 4.1 below, if the entry barrier is low (*e.g.* the

surfactant adsorption layers are incomplete due to low concentration and/or slow kinetics of adsorption). One efficient way to reduce the entry barrier and to transform the oil into a fast antifoam is to add hydrophobic solid particles, and thus to form oil-solid compounds which are considered in section 5. The spreading of the oil makes possible other, non-bridging mechanisms of foam film rupture, which are discussed in section 4.2. Due to the important role of the entry barrier for the antifoam activity and for the specific mode of foam destruction, it is considered separately in section 4.3. In many studies, the antifoam activity is correlated with the so-called entry, E, spreading, S, and bridging, B, coefficients; hence these coefficients are discussed throughout the section, in relation to the various mechanisms of antifoam action.

4.1 Bridging-stretching and bridging-dewetting mechanisms

In this sub-section, we first describe two bridging mechanisms of foam film rupture by oil-based antifoams. Then we discuss the formation and stability of the oil bridges and the related entry and bridging coefficients.

4.1.1 Bridging-dewetting mechanism

This mechanism is often discussed in the literature in relation to oil-based antifoams,[3-6,9,28,32,59-63] by analogy with the foam film rupture by hydrophobic solid particles. The mechanism implies that, once formed, the oil bridges are dewetted by the aqueous phase due to the hydrophobic nature of the oily surface, see Figure 10.12. One should note, however, that in the surfactant solutions with concentration ≥ CMC, the three-phase contact angle θ_{aw} is usually below 90° even for very hydrophobic surfaces.[22,26-28,59-62] Therefore, dewetting of a spherical oil drop is improbable in such solutions, unless the surfactant concentration is low and/or the adsorption is very slow.

In contrast, when the antifoam globule is deformable (oil drop or oil-solid mixture with a large excess of oil), it acquires an equilibrium, non-spherical shape after the first entry into one of the foam film surfaces.[3,8,11,61,69,70] If the three-phase contact angle θ_{aw} (now air-water-oil measured through water) is larger than 90°, the drop acquires the shape of a bi-convex lens, as shown in Figure 10.12(c). Simple geometrical consideration[3] shows that such a lens can be dewetted by the opposite foam film surface at the moment of oil bridge formation, if no significant change of the lens shape occurs during dewetting, Figure 10.12(c)and (d). At the present time, there is no unambiguous evidence that the bridging-dewetting mechanism is operative for oil-based antifoams. However, there are no arguments to discard this possibility (*e.g.* for viscous, non-spreading oils) so that future experiments are expected to clarify this issue.

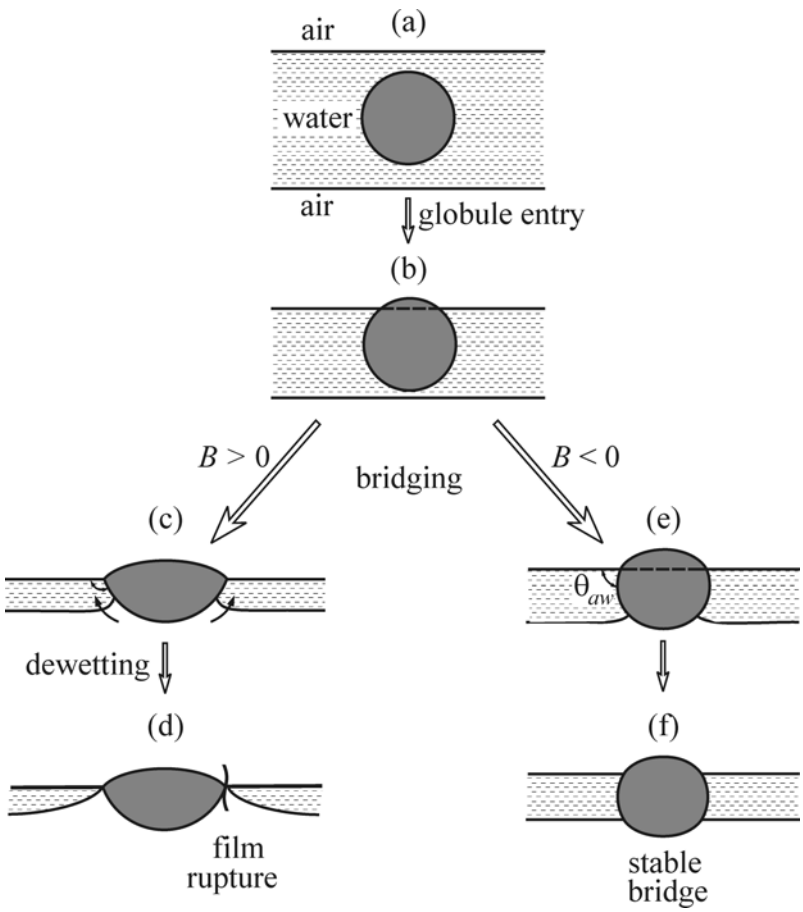

Figure 10.12. Schematic presentation of the bridging of foam film surfaces by an oily globule. (c)-(d) If $B > 0$, the foam film can be ruptured by the bridging-dewetting mechanism or by the bridging-stretching mechanism shown in Figure 10.13. (e)-(f) If the bridging coefficient $B < 0$, the bridge is stable and no film rupture is effected.

4.1.2 Bridging-stretching mechanism

Optical observations with surfactant solutions containing silicone oil-based antifoams showed[8,10] that, once an oil bridge was formed in the foam lamella, it acquired a biconcave shape with the thinnest region being in the bridge center, see Figure 10.13. Such a bridge was unstable due to uncompensated capillary pressures at the oil-water and oil-air interfaces. As a result, the oil bridge spontaneously stretched with time in a radial direction, so that eventually a thin unstable oil film was formed in the bridge center. The rupture of this oil film resulted in the perforation of the entire foam lamella. An important requirement for realization of this bridging-stretching mechanism is the possibility for deformation of the antifoam globule. Therefore, such a mechanism cannot be realized with oil drops which are gelled by polymerization or in the presence of solid particles at high concentration or of inappropriate hydrophobicity.[23] A detailed description of the bridging-stretching mechanism can be found in the original papers[10,11] and in the recent review.[8]

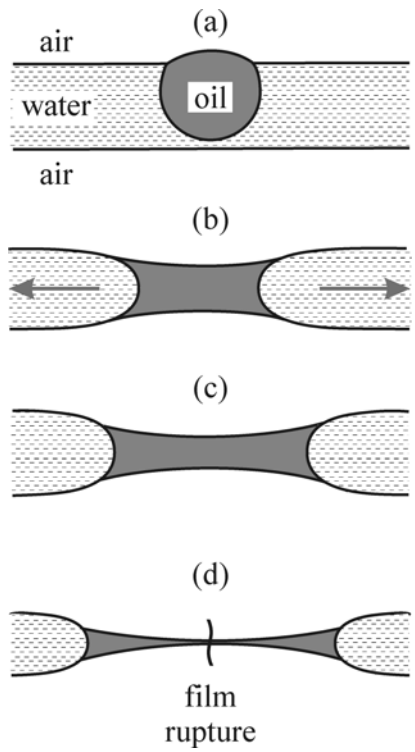

Figure 10.13. Schematic presentation of the bridging-stretching mechanism of foam film rupture by fast antifoams. (a)-(b) Bridging of the foam film surfaces by antifoam globule leads to formation of an oil bridge with non-balanced capillary pressures at the oil-water and air-water interfaces. (c)-(d) The bridge stretches with time until a thin, unstable oil film is formed in the bridge center. The rupture of this oil film leads to destruction of the entire foam lamella.

4.1.3 Entry coefficient

Whatever the mechanism is of foam destruction by antifoam globules, it requires the globules first to enter the solution surface for oil spreading and/or bridge formation to occur. Two different types of factors, thermodynamic and kinetic ones, determine the possibility for realization of drop entry. The thermodynamic aspect is usually discussed in terms of the oil entry coefficient, E, whereas the kinetic aspect is discussed in terms of the drop entry barrier.

The oil entry coefficient[3,61,70] can be calculated from the interfacial tensions of the air-water, γ_{aw}, oil-water, γ_{ow} and oil-air, γ_{oa} interfaces, see Figure 10.14:

$$E = \gamma_{aw} + \gamma_{ow} - \gamma_{oa} \tag{10.16}$$

The value of E depends not only on the used oil but also on the type and concentration of surfactant, electrolyte and co-surfactant, as well as on various other factors which affect the interfacial tensions.

The thermodynamic analysis[3,61,70] shows that negative values of E correspond to complete wetting of the oil drop by the aqueous phase. This means that, even if an oil drop has appeared on the solution surface (*e.g.* as a result of oil deposition from the air phase), this drop would spontaneously immerse into the aqueous phase because this is the thermodynamically

favored configuration, see Figure 10.14(a) and (b). Pre-emulsified oil drops with $E < 0$ remain immersed inside the aqueous phase and cannot form oil bridges between the surfaces of the foam films or Plateau borders. As a result, oils with negative E are inactive as antifoams[3,61,70] (note that $E < 0$ implies that the other two coefficients are also negative, $S < 0$ and $B < 0$). In contrast, positive values of E correspond to a defined equilibrium position of the oil drop/lens at the air-water surface. Hence, when the oil has positive E and the entry barrier is not too high, stable or unstable oil bridges can be formed in the foam films.[3,7,8,61,69]

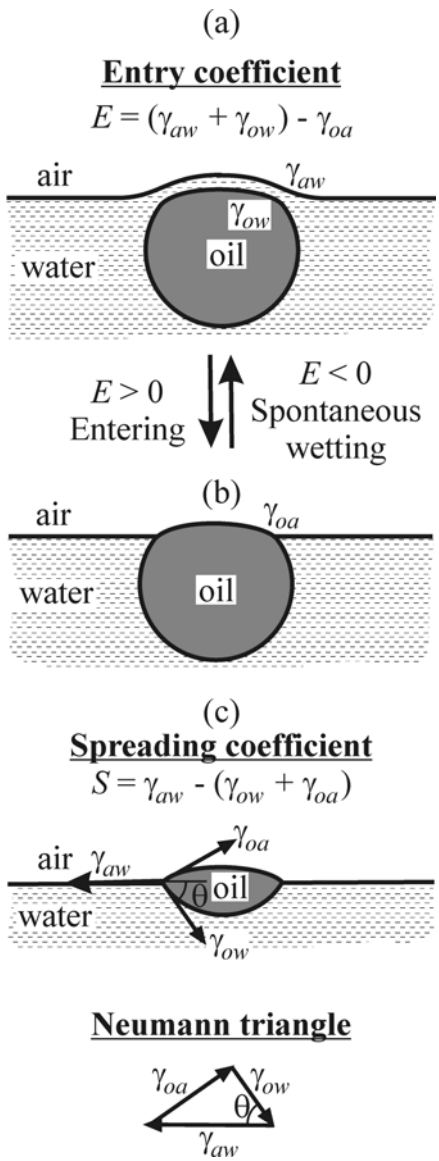

Figure 10.14. Schematic presentation of the meaning of the entry, (a) and (b), and spreading (c) coefficients.

To illustrate the relation between the entry coefficient, E, and the entry barrier, let us draw an analogy with the concepts used in chemical kinetics. A positive value of E is the thermodynamic condition for the existence of an equilibrium position of the oil drops at the air-water surface and for formation of oil bridges in the foam films, whereas the entry barrier plays

the role of a kinetic barrier which can preclude the realization of these thermodynamically favored configurations, *viz*. the oil drop can remain arrested in the aqueous phase for kinetic reasons.

4.1.4 Stability of oil bridges in foam films - bridging coefficient

The first theoretical study of the stability of oil bridges in foam films in relation to antifoaming was made by Garrett.[69] He analyzed the conditions for mechanical equilibrium of an oil bridge, which is placed in a foam film with perfectly planar surfaces, see Figure 10.15. The mechanical equilibrium of such a capillary system requires the balance of (i) the capillary pressures across the various interfaces and (ii) the interfacial tensions acting on the three-phase contact lines. The second balance can be expressed by the Neumann triangle, illustrated in Figure 10.14(c).

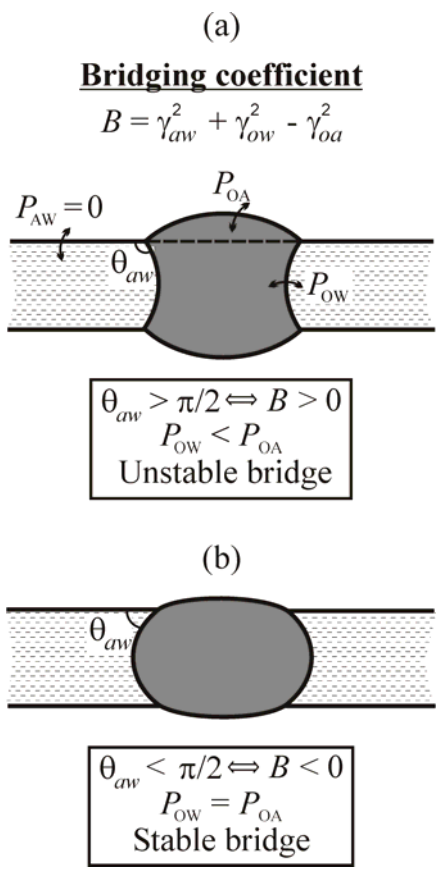

Figure 10.15. Schematic presentation of an oil bridge in a foam film with planar surfaces according to Garrett's model.[3,69] (a) Unstable bridge with positive bridging coefficient, $B > 0$ ($\theta_{aw} > 90°$) and (b) stable bridge with negative bridging coefficient, $B < 0$ ($\theta_{aw} < 90°$).

To assess the oil bridge stability, Garrett checked whether the capillary pressures across the oil-air and oil-water interfaces ($P_{oa} \equiv P_o - P_a$ and $P_{ow} \equiv P_o - P_w$) and the Neumann triangle at the bridge periphery can be simultaneously balanced, Figure 10.15. The analysis showed that if the contact angle $\theta_{aw} > \pi/2$, the capillary pressure P_{ow} is always smaller than P_{oa}. In other words,

it is impossible to achieve mechanical equilibrium of an oil bridge with $\theta_{aw} > \pi/2$. Such bridges are considered unstable and they rupture the foam films by either of the bridging mechanisms discussed above, Figure 10.15(a). In contrast, when $\theta_{aw} < \pi/2$, both the Neumann triangle and the pressure balance can be satisfied, so that the respective oil bridges are mechanically stable and no antifoam effect of the oil is expected, Figure 10.15(b).

By applying the cosine theorem to the Neumann triangle, Garrett[69] proved that the requirement $\theta_{aw} > \pi/2$ is equivalent to the condition

$$B \equiv \gamma_{aw}^2 + \gamma_{ow}^2 - \gamma_{oa}^2 > 0 \tag{10.17}$$

where B is the bridging coefficient. It can be shown theoretically that positive values of B necessarily mean positive entry coefficient, E, while the reverse statement is not always true.[37,70] In conclusion, Garrett's analysis predicts that oils with $B > 0$ would form unstable bridges and *vice versa*.

An important assumption in Garrett's model is that the surfaces of the foam film are perfectly planar. A more complex model, which accounts for the possible deformation of the foam film surfaces by the oil bridge, was developed in ref. 11. This model revealed that the bridge stability and shape depend not only on the contact angle θ_{aw}, but also on the bridge volume, V_B. Another important conclusion of this model was that the oil bridges could acquire equilibrium shapes (satisfying Neumann triangle and balanced capillary pressures), for both positive and negative values of B. These equilibrium shapes usually include a certain deformation of the foam film surfaces not accounted for in Garrett's model. As an illustration, Figure 10.16(a) and (b) shows theoretically calculated equilibrium shapes of two oil bridges with $\theta_{aw} = 130°$ and 73°, respectively. Note that the equilibrium bridge shown in Figure 10.16(a) is with $\theta_{aw} > 90°$, which corresponds to $B > 0$.

The theoretical analysis in ref. 11 revealed that some of the bridge shapes describe stable equilibrium configurations, whereas other shapes describe unstable equilibrium configurations, corresponding to a local maximum of the system energy. Therefore, the complete theoretical analysis of foam film stability in the presence of oil bridges requires one to clarify the domains of stable and unstable equilibrium bridges. The numerical calculations showed[11] that the bridge stability depends mainly on two factors: the value of θ_{aw} and the ratio V_B/V_0, where $V_0 = (\pi h^3/6)$ is the volume of an imaginary oil drop with diameter equal to the film thickness. As seen from Figure 10.16(c), only stable bridges exist at $B < 0$, in accordance with Garrett's prediction.[69] However, both stable and unstable equilibrium bridges can be formed at $B > 0$. The large bridges are always unstable, whereas the small bridges could be stable or unstable, depending on the value of θ_{aw}.[11]

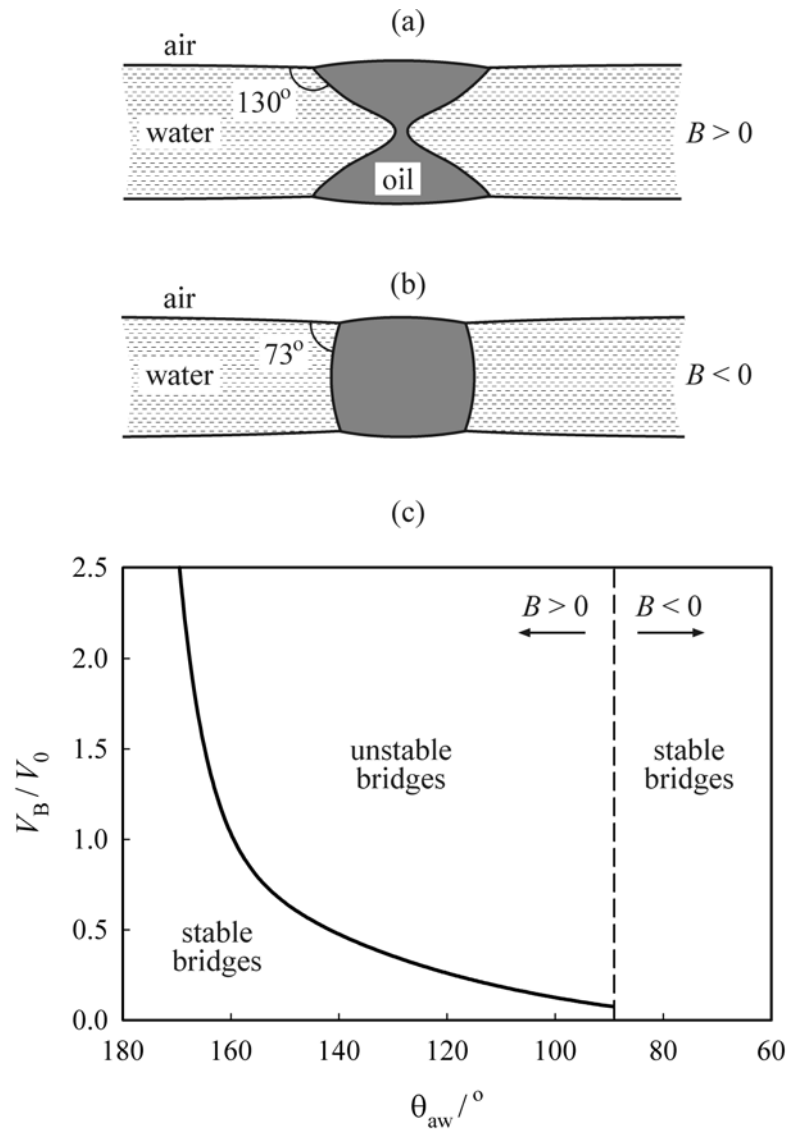

Figure 10.16. Equilibrium shape of oil bridges with different air-water-oil contact angles being (a) 130° and (b) 73°. (c) The dimensionless bridge volume, V_B/V_0, plotted as a function of the contact angle θ_{aw}, where $V_0 = (\pi h^3/6)$. The remaining parameters in the calculations are γ_{oa} = 20.6 mN m^{-1}, γ_{ow} = 4.7 mN m^{-1} and h = 2 μm. Adapted from ref. 11.

4.2 Role of oil spreading in antifoam activity

4.2.1 Spreading coefficient

The spreading affinity of oils is usually discussed in terms of their spreading coefficients, see Figure 10.14(c).[3,60-62,70,71]

$$S = \gamma_{aw} - \gamma_{ow} - \gamma_{oa} \tag{10.18}$$

It is important to distinguish between the initial spreading coefficient, S_{IN} (defined by using γ_{aw} in the absence of spread oil on the solution surface) and the equilibrium spreading coefficient, S_{EQ} (γ_{aw} in the presence of spread oil).[3,61,70] Rigorous thermodynamic analysis shows that $S_{EQ} \leq 0$, while S_{IN} might have arbitrary sign (see refs. 3, 61 and 70 for more explanation). Note that $S_{EQ} \leq S_{IN}$ because γ_{aw} decreases upon oil spreading.

The signs of S_{IN} and S_{EQ} bring direct information about the spreading behavior of the oils. The initial spreading affinity, after the oil is first deposited on the solution surface, is characterized by S_{IN}. Negative value of S_{IN} means that the oil does not spread on the surface. Positive S_{IN} means that the oil would spread as a thin or thick layer. Likewise, S_{EQ} brings information about the thickness of the equilibrium spread layer: if $\gamma_{aw} = \gamma_{ow} + \gamma_{oa}$ (*i.e.* $S_{EQ} = 0$), the Neumann triangle predicts $\theta_{aw} = 0$ and the oil spreads as a thick layer (so-called "duplex film"), whereas negative S_{EQ} and positive S_{IN} imply a thin equilibrium layer, possibly co-existing with oil lenses. The comparison of equations 10.16 and 10.18 shows that if $S > 0$, the entry coefficient is also positive, $E > 0$, because $(E - S) = 2\,\gamma_{ow} > 0$.

4.2.2 Relation between oil spreading and antifoaming

The first study relating the antifoam effect of oils with their spreading behavior was published by Ross.[72] He found that most of the oils with noticeable antifoam activity had positive spreading coefficients. Since that time, there has been an ongoing debate in the literature about the role of oil spreading in the antifoam mechanisms, *e.g.* see refs. 3-17, 22, 28, 32, 54, 59-65, 70, 73-78. The discussions are usually made in the context of the assumed mode of antifoam action. Ross[72] speculated that the oil should first connect the two foam film surfaces (*i.e.* an oil bridge is formed) and then spread as a thick layer, in order to replace a portion of the stable aqueous foam film by an unstable oil bridge so that the film rupture can occur. Later experimental studies[3,32] showed that foam film rupture through oil bridge formation is possible at negative values of S_{EQ} and S_{IN}, which means that there is no specific requirement for spreading of the oil as a thick layer (note that the theoretical analysis of the oil bridge stability requires $B > 0$ without imposing any requirement for the spreading behavior of the oil). In other words, oil spreading is not a necessary condition to have antifoam activity of the oils and oil-based compounds.[3,8,10,32] Nevertheless, the correlation between the spreading ability of the oils and their antifoam activity, which is observed in many systems, suggests that the spreading could either facilitate the foam destruction process by some of the bridging mechanisms discussed in section 4.3 or induce another non-bridging mechanism of foam destruction.

Several non-bridging mechanisms were proposed in the literature. The "spreading-fluid entrainment" mechanism[3,28] implies that once an oil drop with positive S_{IN} enters either of the foam film surfaces, the oil spreads in a radial direction from the formed oil lens. This spreading is assumed to drag water in the foam film away from the oil lens, inducing in this way local film thinning and subsequent rupture. Several theoretical models based on this idea were published in

the literature, but this mechanism has not found unequivocal confirmation in experimental studies.

In other studies, oil spreading on the surfaces of foam films was directly observed and related to the film rupture.[8,14,15] These observations showed that the spreading oil induces capillary waves of large amplitude on the surface of the foam films (Δh ~ hundreds of nanometers). These waves covered almost the entire foam film and often led to film rupture within several seconds, even at relatively large average film thickness $h \approx 1$ μm. As discussed in ref. 8, the spreading oil probably "sweeps" some of the surfactant adsorbed on the foam film surface, which results in film destabilization for two main reasons.[8] First, the induced capillary waves (related to the decreased surface elasticity and viscosity of the diluted surfactant adsorption layers) lead to the formation of locally thin regions in the film, which allows film rupture at relatively large average thickness. Second, the diluted adsorption layers cannot stabilize efficiently the local thin spots against rupture, due to the reduced surface charge density on the film surfaces (hence suppressed electrostatic repulsion) and/or to the appearance of attractive hydrophobic forces.[35,37] This mode of foam film rupture was termed "spreading-wave generation" mechanism of antifoam action.[8]

An additional factor for capillary wave generation and foam film destabilization could be the asymmetric surfactant distribution which appears after the oil spreads on only one of the foam film surfaces (see Figure 10.17 for schematic presentation and ref. 59 for experimental results), which is the typical case in defoamer applications. As shown by Binks *et al.*,[78] foam destabilization can be induced by oil vapour which adsorbs first on only one of the foam film surfaces. Then the oil molecules diffuse across the foam films to establish an equilibrium distribution of the oil and surfactant molecules on both surfaces of the foam films. Ivanov, Danov and co-workers,[79-81] showed experimentally and analyzed theoretically that the diffusion of surface active substances across liquid films could induce film rupture by a Marangoni type of instability.

Let us mention several possible effects of oil spreading on the bridging modes of antifoam action. As shown in ref. 22, oil spreading on the foam film surfaces can facilitate the bridging mechanisms by (i) reducing the entry barriers of the emulsified antifoam globules, (ii) facilitating the antifoam dispersion inside the foaming solution, thus increasing the number concentration of the antifoam globules and (iii) facilitating the oil bridge rupture by supplying oil which increases the bridge volume V_B above the critical value separating the stable from unstable bridges (see Figure 10.16(c)). Detailed explanations of all these effects can be found in ref. 8.

The above discussion shows that a positive spreading coefficient, S_{IN}, and high spreading rate, which effectuate the oil spreading during foaming, could enhance significantly the antifoam activity without being a necessary pre-requisite for antifoam action.

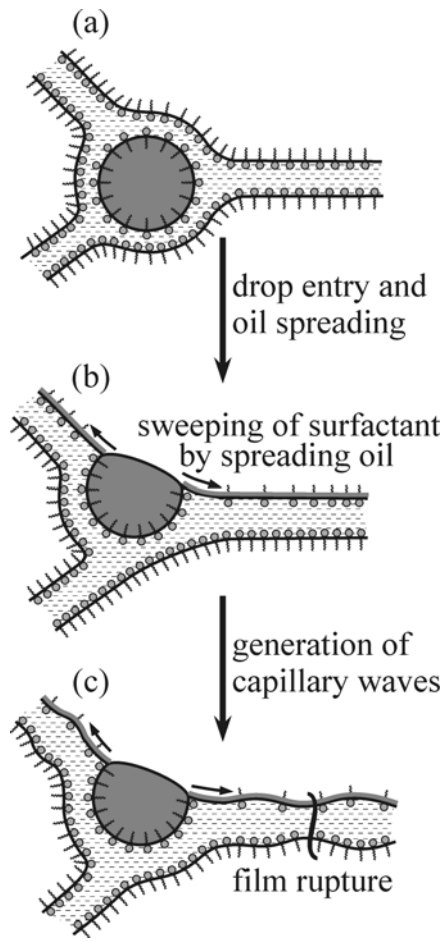

Figure 10.17. Schematic presentation of the "spreading-wave generation" mechanism. (a)-(b) Entry of an oil drop in the region of the Plateau channel leads to oil spreading on the surfaces of the neighboring foam films. (b)-(c) The spreading oil partially sweeps the surfactant from one of the film surfaces leading to the appearance of capillary waves. The local thinning of the foam film and the loose adsorption layer lead to foam film rupture.

4.3 Role of entry barrier for the activity of oil-based antifoams

In this sub-section we first define the entry barrier and explain the experimental method for its measurement. Then, several important results relating the magnitude of the entry barrier to the antifoam activity are discussed.

4.3.1 Film Trapping Technique for measuring the entry barrier

Several definitions of the entry barrier were proposed in the literature, which are related to the experimental or theoretical methods used for its determination. Recently, the Film Trapping Technique (FTT) was developed[16,18] for quantifying the entry barrier of oil drops and mixed oil-solid antifoam globules. In this technique, the capillary pressure of the air-water surface is measured at the moment of drop/globule entry, $P_C^{CR} = (P_a - P_w)$, see Figure 10.18.

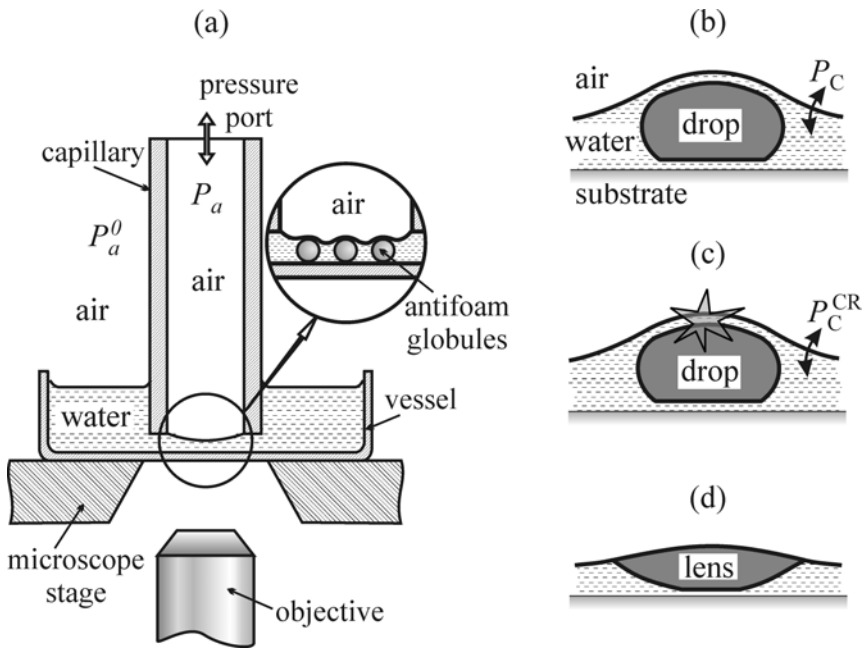

Figure 10.18. Scheme of the experimental setup and the principle of operation of the Film Trapping Technique (FTT).[18] (a) and (b) Vertical capillary partially immersed in surfactant solution containing oil drops is held close above the bottom of the experimental vessel. The air pressure inside the capillary, P_a, is increased and the air-water meniscus in the capillary is pressed against the glass substrate. Some of the oil drops remain trapped in the wetting glass-water-air film and are compressed by the meniscus. (c) At a certain critical capillary pressure, $P_C^{CR} = (P_a - P_w)$, the asymmetric film formed between the oil drop and the solution surface ruptures and the drop enters the air-water surface forming a lens (d).

The use of P_C^{CR} as a characteristic of the entry barrier provides several important advantages in comparison with the other quantities used in literature for this purpose. First, P_C^{CR} has a clear physical interpretation with respect to the antifoam action – it corresponds to the capillary pressure which compresses the oil drops in the actual foam (by the surfaces of the thinning foam film or by the walls of shrinking Plateau borders) at the moment of drop entry. Thus the value of P_C^{CR} can be related to foam properties, such as foam height, bubble size, rate of water drainage, which affect the capillary pressure in real foams. Second, P_C^{CR} can be measured by the FTT for oil drops of micrometer size, possibly containing solid particles, like those encountered in practical systems. Therefore, no additional hypotheses are needed to transfer the conclusions from the model FTT experiments to real foams. Third, it allows one to study the effect on the entry barrier of various important factors, such as globule size, oil spreading and hydrophobicity and concentration of solid particles in the antifoam compounds. Last but not least, the FTT requires inexpensive equipment and an experienced operator can obtain a large set of data in a relatively short period of time.

4.3.2 Role of entry barrier for the general mode of antifoam action

The application of the FTT to various antifoam-surfactant systems has shown that the entry barrier, P_C^{CR}, plays a key role in the antifoam activity and in determining the specific mode of antifoam action.[8,13,16,18-24] In Figure 10.19, we show summarized results for the foam half-life as a function of P_C^{CR} for various surfactant-antifoam pairs. One sees that the data fall into two distinct regions: (i) Systems in which the foam was destroyed in less than 10 seconds and the entry barrier was always below 15 Pa, (ii) systems in which the foam half-life was longer than 5 minutes and the entry barrier was above 20 Pa. These results show that there is a threshold value of the entry barrier, $P_{TR} \approx 15$ Pa, which separates the two distinct domains of foam half-life. Microscope observations showed that, if $P_C^{CR} < P_{TR}$, the antifoam globules are able to easily enter the solution surface and to break the foam films in the early stages of their thinning, *i.e*. the antifoam acts as a fast one.[8,10,19] In contrast, if $P_C^{CR} > P_{TR}$, the antifoam globules are expelled from the films into the neighboring Plateau borders, *i.e*. the antifoam acts as a slow one.[8,14-18]

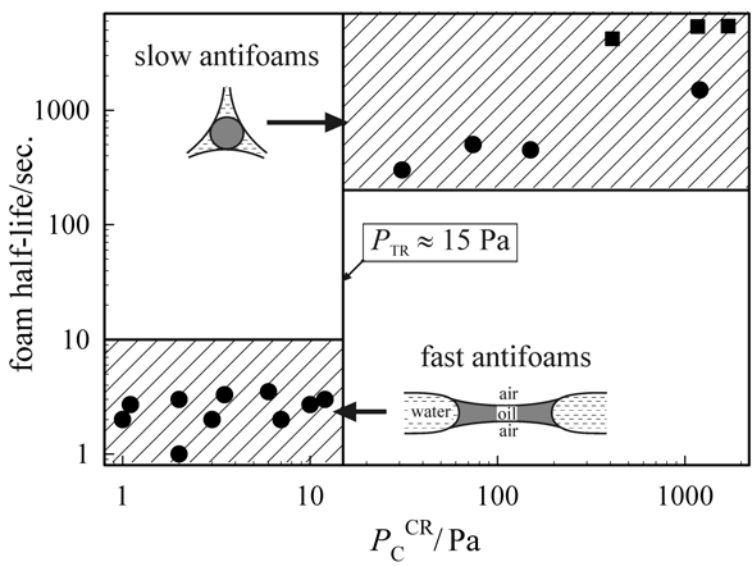

Figure 10.19. Foam half-life, $t_{1/2}$, as a function of drop entry barrier, P_C^{CR}, for different surfactant-antifoam pairs (see ref. 16 for their description). Note the logarithmic scale on the axes. Adapted from ref. 16.

4.3.3 Role of entry barrier and drop size for the activity of slow antifoams

Here, as another example of the important role of the entry barrier for the antifoam activity, we explain theoretically the height of the residual foam, H_{RES}, which is observed experimentally in the presence of slow antifoams, see section 2.3 and stage IV in Figure 10.9(a).[14,16] On this basis, we discuss the role of co-surfactants, which are used as foam boosters in the presence of oily antifoams.

Let us consider a foam column with height $H_F(t)$ which contains oil drops with mean radius R_D and entry barrier, P_C^{CR}. From equations 10.2-10.4 one can calculate the equilibrium cross-sectional radius of the PBs, R_{CS}, and the respective capillary pressure, P_C^{PB}, at the top of the foam column (*i.e.* at $Z = H_F$) where the PBs are narrowest and the pressure is highest:

$$R_{CS}(H_F) \approx 0.155 \frac{\gamma_{aw}}{\rho g H_F} \tag{10.19}$$

$$P_C^{PB}(H_F) \approx \rho g H_F \tag{10.20}$$

Equations 10.19 and 10.20 predict that at equilibrium, $P_C^{PB} \approx 10^3$ Pa and $R_{CS} \approx 5$ μm for a foam column with height $H_F = 10$ cm, whereas $P_C^{PB} \approx 100$ Pa and $R_{CS} \approx 50$ μm for $H_F = 1$ cm ($\gamma_{aw} = 30$ mN m^{-1} and $\rho \approx 10^3$ kg m^{-3} are used in these estimates). Therefore, P_C^{PB} decreases and R_{CS} increases when the foam column decreases its height, *e.g.* as a result of antifoam induced decay.

If the oil drops trapped in the PBs of the initially formed foam with height H_{F0} have entry barrier $P_C^{CR} < P_C^{PB}(H_{F0})$ and radius $R_D > R_{CS}(H_{F0})$, then foam destruction would begin after a certain period of water drainage because the asymmetric oil-water-air films formed between the trapped oil drops and the walls of the Plateau channels (see Figure 10.9(c)) would be unable to resist the compressing capillary pressure. The foam destruction would continue until the foam height becomes so small that $P_C^{PB}(H_F) \approx P_C^{CR}$ (*i.e.* the asymmetric films become stable) or the cross-section of the Plateau channels becomes approximately equal to the drop size, $R_{CS}(H_F) \approx R_D$ (*i.e.* the oil drops are not compressed anymore by the PB walls, Figure 10.9(d)). Hence, the height of the residual foam can be evaluated from the relation $H_{RES} \approx \max\{H_P, H_R\}$, where

$$H_P = \frac{P_C^{CR}}{\rho g} \tag{10.21}$$

$$H_R = 0.155 \frac{\gamma_{aw}}{\rho g} \frac{1}{R_D} \tag{10.22}$$

One can use the dimensionless ratio

$$\frac{H_P}{H_R} = \frac{P_C^{CR} R_D}{0.155\, \gamma_{aw}} \tag{10.23}$$

to determine whether H_{RES} is governed by the entry barrier of the oil drops or by their size. If $(H_P/H_R) > 1$, which corresponds to large drops and/or high entry barrier, H_{RES} is determined by the entry barrier. In this case, the oil drops are compressed but the asymmetric films are stable. In contrast, if $(H_P/H_R) < 1$ (*i.e.* for small drops and/or low barrier), H_{RES} is determined by the drop size while the entry barrier is not important because the oil drops are too small to be compressed at the end of the foam destruction process.

The relevance of the above estimates to real foams was verified by comparing the predictions of equations 10.21-10.23 to experimental results obtained with a series of surfactant-

antifoam pairs.[16] The entry barrier, P_C^{CR}, was measured by the FTT, H_{RES} was measured by foam test and the oil drop size was determined by optical microscopy. As expected, at high entry barriers, $P_C^{CR} \geq 400$ Pa, corresponding to taller foam columns, $H_{RES} \approx H_P$; see the continuous line in Figure 10.20 which is drawn according to equation 10.21 without any adjustable parameter. At lower entry barriers, $P_C^{CR} < 400$ Pa, the final foam height $H_{RES} \approx H_R$ was independent of P_C^{CR}; see the experimental points below the horizontal dashed line in Figure 10.20, because the Plateau channels were too wide to compress the emulsified oil drops in the respective short foam columns.

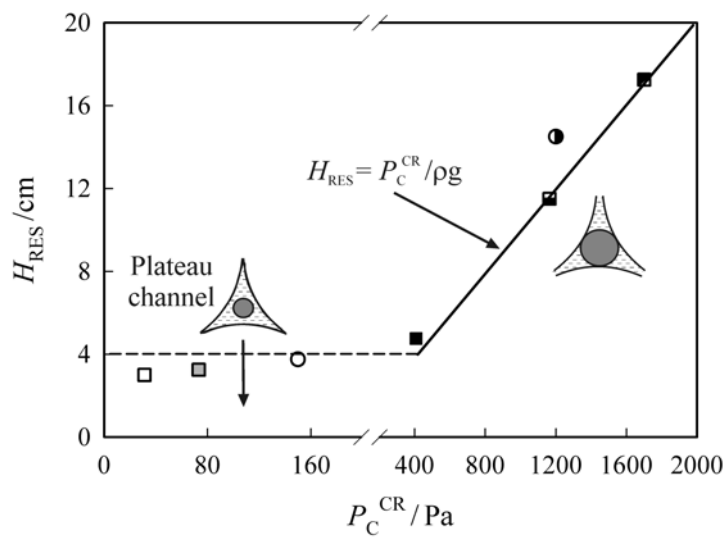

Figure 10.20. Experimental results (symbols) for the height of the residual foam H_{RES} (from Ross-Miles test) *versus* the entry barrier P_C^{CR} measured by the FTT with different surfactant-co-surfactant mixtures containing 0.1 wt. % silicone oil as a slow antifoam. The continuous line is a theoretical estimate from equation 10.21. Adapted from ref. 16.

Equations 10.21 and 10.22 predict that one can vary the entry barrier and/or the oil drop size to control the final foam height in the presence of slow antifoams. Indeed, FTT measurements[14-16] showed that the addition to the main surfactant of different co-surfactants, such as dodecanol, betaines and aminoxides, led to a significant increase in the oil drop entry barrier at fixed total surfactant concentration. In agreement with equation 10.21, enhanced foam stability was found in the foam tests,[14,15] see Figure 10.21(a). In complementary experiments, the foam stability was found to be higher when the oil was dispersed into smaller drops (at fixed composition of the surfactant solution), as predicted by equation 10.22; see Figure 10.21(b) for illustrative results. Therefore, one can use appropriate co-surfactants as foam boosters which improve the foam stability by increasing the entry barrier and/or by facilitating the emulsification of the antifoam into smaller drops. For enhancing the foaminess of the respective solutions, faster kinetics of surfactant adsorption is also essential.

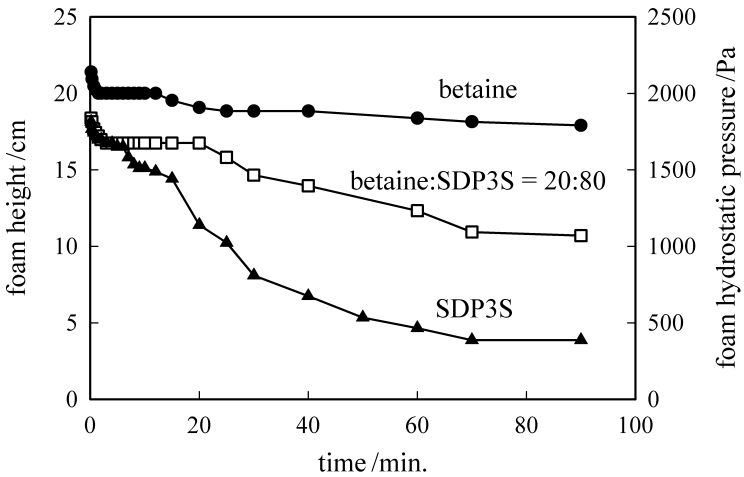

(a)

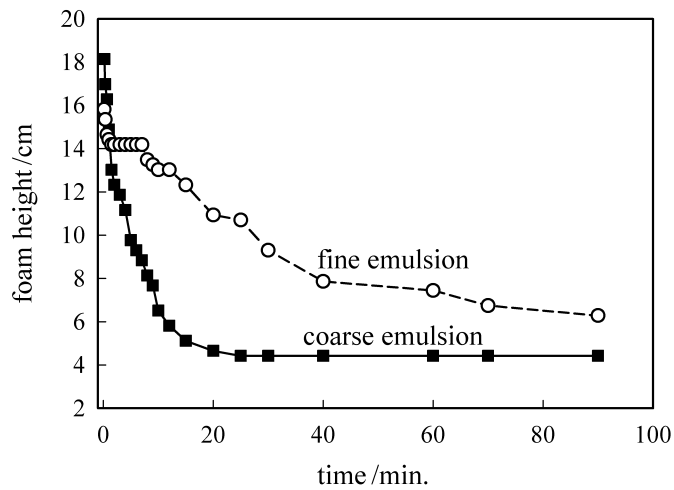

(b)

Figure 10.21. (a) Effect of betaine (co-surfactant used as foam booster) on foam stability in the presence of 0.1 wt. % silicone oil as a slow antifoam. The primary surfactant is the anionic SDP3S and the total surfactant concentration is 0.1 M. The left-hand-side axis shows the foam height and the right-hand-side axis shows the respective hydrostatic pressure, at the top of the foam column. As verified by FTT, the main role of betaine is to increase the drop entry barrier, which was measured to be very similar to the hydrostatic pressure of the residual foam (after 70 min): $P_C^{CR} \approx 400$ Pa for SDP3S, ≈ 1100 Pa for the surfactant mixture, and higher than 2000 Pa for betaine. (b) Effect of oil drop size on foam stability for a 0.1 M SDP3S solution. Adapted from ref. 14.

5 Mixed oil-solid compound antifoams

In this section we first explain the observed synergistic effect between oil and solid particles in antifoam compounds. The discussion is focused on those properties of oils and particles which are essential for their synergistic action. Then, we describe the mechanism of compound exhaustion which is closely related to the oil-particle synergy.

5.1 Synergistic antifoam action of oil and solid particles

The strong synergistic effect between oil and solid particles often observed with antifoam compounds is related to the complementary roles of these two components. The main role of the solid particles is to destabilize the asymmetric oil-water-air films, facilitating in this way the oil drop entry ("pin-effect" of the solid particles).[3,5,10,16,19,23,28,32,54,59-61,82-86] Another important role of the solid particles is to increase the so-called "penetration depth" of the oil lenses floating on foam film surfaces, which facilitates oil bridge formation in thicker foam films.[6,11,54,63]

The main role of the oil is to ensure deformability of the compound globules, which is an important requirement for foam film rupture by the bridging-stretching mechanism and in many cases by the bridging-dewetting mechanism. In addition, oil spreading could facilitate the entry of the antifoam globules and the foam film rupture as discussed in sections 4.2 and 5.2. In mineral and ore flotation, where no strong surfactants are used and the solid particles are usually in excess with respect to the oil, the latter could increase the hydrophobicity of the particles by coating them with a thin layer of oil.[63]

5.2 Effect of solid particles and spread oil on the formation and stability of oil bridges

5.2.1 Pin effect of solid particles

The pin effect of the solid particles on the entry barrier of compound globules is illustrated in Table 10.1 with data obtained by the FTT.[16,21-24] Comparative experiments were performed with drops of silicone oil (without silica) and with globules of silicone oil + silica in solutions of two different surfactants. To clarify the effect of oil spreading on the entry barrier, two types of experiments were performed for each system - with and without a pre-spread layer of silicone oil.

The data in Table 10.1 show that the entry barrier is strongly reduced by the presence of hydrophobic silica in the compound globules (see also Figure 10.22). The mechanistic explanation of the "pin effect" (both in the presence and in the absence of spread oil) can be given by using the concepts from section 3.2, where we discussed the antifoam effect of solid particles with sharp edges. In accordance with the Derjaguin approximation, equation 10.13, small solid particles of nanometer size and/or having sharp edges adsorbed on the surface of the oil drop (Figure 10.23) can come into direct contact with the foam film surface much easier than the drop surface itself, because a repulsive force of lower magnitude has to be overcome.[3] For typical silica agglomerates of fractal shape used in antifoam compounds, one can approximate R_P in equation 10.13 by the radius of the primary silica particles, ~ 5 nm, which is three orders of magnitude smaller than the typical size of the antifoam globules, ~ 5 μm. Hence, if a compound globule is pushed against the foam film surface by a hydrodynamic force, the solid particles would come into direct contact with the film surface and will form solid bridges at much lower force, as compared to the entry of the same oil drop without solid inclusions. The pin effect leads

to the formation of solid bridges between the oil globule and the foam film surface, see Figure 10.23(b). If the solid particles are sufficiently hydrophobic, these solid bridges lead to oil emergence on the film surface, *viz*. particle-aided entry of the oil globule.

Table 10.1 Entry barriers, P_C^{CR}, of different antifoams in 10 mM AOT and 1 mM Triton X100 solutions in the presence and in the absence of a pre-spread layer of silicone oil. In foam tests, both compounds behave as a fast antifoam, the silicone oil acts as a slow antifoam whereas the reference surfactant solutions (without antifoam) are stable. The difference between the silicone oil+silica samples 1 and 2 is explained in ref. 22, where the data are taken from.

Antifoam	**Spread layer**	**AOT**	**Triton X100**
		P_C^{CR}/Pa	
silicone oil	No	28 ± 1	>200
	Yes	19 ± 2	> 200
(silicone oil+silica) - 1	No	8 ± 1	30 ± 1
	Yes	3 ± 2	5 ± 2
(silicone oil+silica) - 2	No	20 ± 5	22 ± 1
	Yes	4 ± 1	7 ± 1

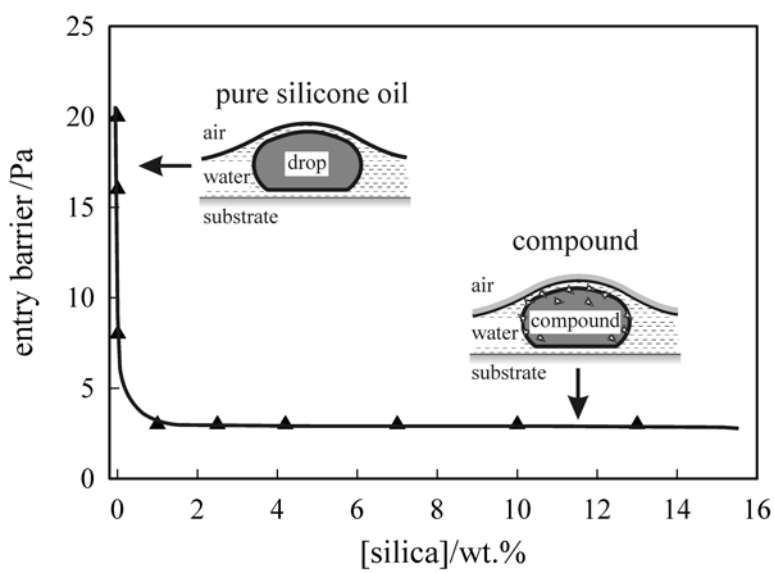

Figure 10.22. Dependence of the entry barrier of silicone oil + silica compound globules on the silica particle concentration in the compound. The entry barrier is measured by the FTT in 10 mM AOT solution. Adapted from ref. 24.

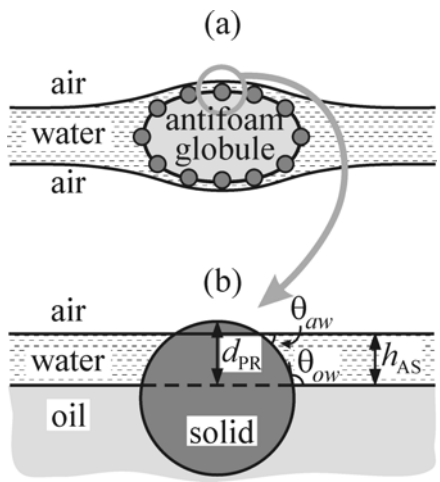

Figure 10.23. (a) When an antifoam globule of oil and particles is trapped in a foam film, asymmetric oil-water-air films are formed. (b) If the protrusion depth, d_{PR}, of the solid particles is larger than the thickness of the asymmetric film, h_{AS}, and the condition for dewetting is satisfied, the solid particle pierces the air-water surface and induces rupture of the asymmetric film (*i.e*. the solid particle assists the oil globule entry).

5.2.2 Effect of particle hydrophobicity

To test how the antifoam performance and the entry barrier of mixed globules of silicone oil + silica particles depend on the hydrophobicity of the particles, the following procedure for compound preparation was used.[21,23] Hydrophilic particles were mixed with silicone oil (PDMS) at room temperature and this mixture was stored for months under mild stirring. During this period, PDMS molecules slowly adsorbed on the silica surface rendering it more hydrophobic with time. In parallel experiments, spherical glass beads of millimeter size were hydrophobized by the same procedure and their hydrophobicity was assessed by measuring the particle contact angle at the PDMS-surfactant solution interface.[22,26] As seen from Figure 10.24, the hydrophobization process is very slow at room temperature which allows one to study the effect of silica hydrophobicity on the antifoam activity of the compounds.[21,23]

The FTT experiments showed a pronounced minimum of the entry barrier, P_C^{CR} as a function of the silica particle hydrophobicity,[21,23] which corresponded to a maximum in the compound durability, Figure 10.24(b). These results point to the presence of an optimal silica hydrophobicity for best antifoam performance. The observed minimum in P_C^{CR} was explained by a combination of two opposite requirements for the silica particles.[8,23] The first requirement is that the solid particles should protrude sufficiently deep into the aqueous phase in order to bridge the surfaces of the asymmetric oil-water-air film formed between the oil globule and the foam film surface. The protrusion depth of solid spheres can be estimated from the expression $d_{PR} = R_P(1+\cos\theta_{ow})$, where R_P is the particle radius and θ_{ow} is the contact angle oil-water-solid measured into the aqueous phase, Figure 10.23(b). One sees that deeper protrusion is ensured by more hydrophilic particles.

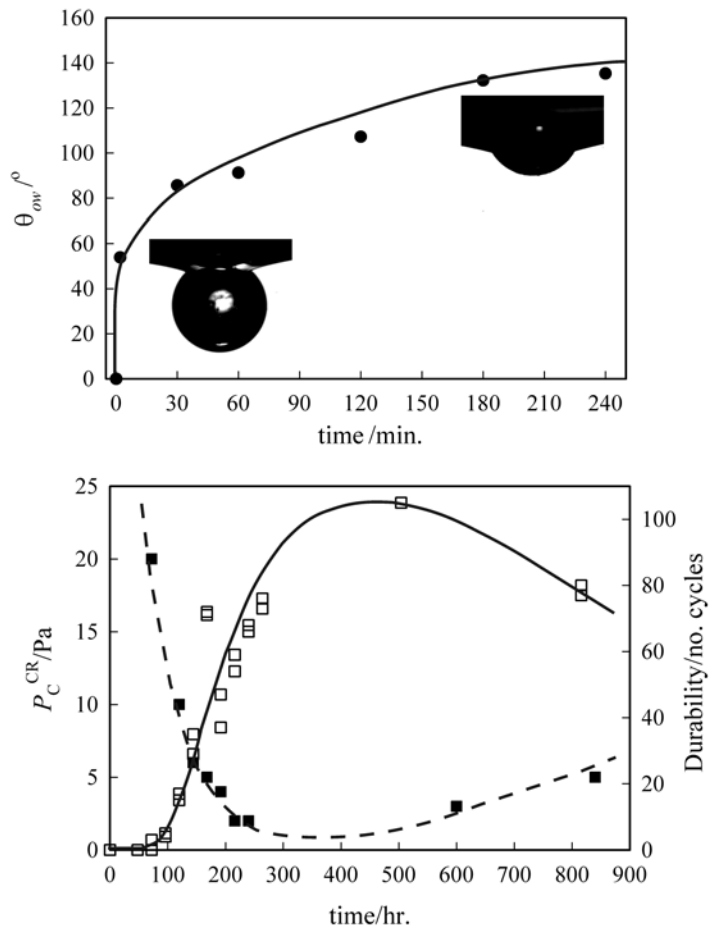

Figure 10.24. (a) Three-phase contact angle measured through water of spherical glass particles attached to the interface between a 10 mM AOT solution and silicone oil as a function of the time of contact of the particles with oil (*viz*. the time for hydrophobization of the particle surface by adsorption of silicone oil molecules). The images show photographs of the respective particles. (b) Critical pressure for globule entry, P_C^{CR} (full squares) and durability (empty squares) of silicone oil + silica compound in 10 mM AOT solution as a function of the time of silica hydrophobization. Adapted from ref. 23.

The second requirement[3,61] is that the particles should be sufficiently hydrophobic to be dewetted by the oil-water and air-water interfaces in order to induce globule entry. For complete dewetting of a spherical particle to occur, the three-phase contact angles θ_{ow} and θ_{aw} formed at the two contact lines (Figure 10.23(b)) should satisfy the condition

$$\theta_{\mathrm{ow}} + \theta_{\mathrm{aw}} > 180^{\circ} \qquad \text{unstable asymmetric film} \qquad (10.24)$$

Therefore, if a solid bridge is formed and condition 10.21 is satisfied, the oil from the drop "uses" the bridge to come into direct contact with the foam film surface. In contrast, when (θ_{ow} + θ_{aw}) < 180°, there are well defined equilibrium positions of the three-phase contact lines on the particle surface such that the particles can even stabilize the oil-water-air film against rupture.[61]

The two opposite requirements described above explain why an optimal hydrophobicity of the solid particles in compounds would ensure lowest entry barrier. For spherical particles, the

optimal contact angle can be estimated by assuming that the particle protrusion depth, d_{PR}, should be equal to the equilibrium thickness of the asymmetric oil-water-air film, h_{AS} (note that the films between the antifoam globules and the foam film surface are usually of micrometer size and thin very rapidly so that the kinetics aspects are not important here)[21]

$$\cos\theta_{ow} \approx h_{AS} / R_P - 1 \tag{10.25}$$

which predicts that the optimal contact angle decreases with an increase in h_{AS} and with a decrease in particle size. The above mechanistic approach for analyzing the effect of solid particles on the entry barrier of compound globules was further developed to include the case with a spread oil layer on the foam film surfaces.

5.2.3 Effect of the spread oil on the entry barrier of compound globules

The experimental data shown in Table 10.1 show that all entry barriers of the studied oil + silica compounds were reduced in the presence of spread oil and were well below the threshold value separating the fast from slow antifoams, $P_{TR} \approx 15$ Pa, which is in agreement with their high antifoam activity observed in the foam tests.[22,23] In Triton X100 nonionic surfactant solutions, the barriers were even higher than the value of P_{TR} in absence of spread oil. The most important and non-trivial conclusion from all these data is that the fast antifoam action observed with the studied compounds in Triton X100 solutions is due to the combined action of the solid particles in the globules and the spread oil layer on the solution surface. Without spread oil, the entry barrier would be too high to allow fast antifoam action. In the following, we give a mechanistic explanation of the effect of spread oil on the entry barrier of compound globules.

Since the repulsive barrier between the small solid particles and the solution surface is always expected to be low due to the particle pin effect, one can expect that the spread oil does not affect significantly the conditions for formation of the solid bridges between the compound globules and the foam film surfaces. However, the conditions for dewetting of the solid bridges formed change in the presence of spread oil, as shown by optical observations and theoretical analysis in ref. 22. Once a hydrophobic solid particle comes into direct contact with the air-water surface covered by a spread oil layer, the oil starts to accumulate in the area of the contact line forming an oil collar, see Figure 10.25. This process is driven by the particle hydrophobicity and is energetically favored to displace the aqueous phase contacting the particle surface by oil. The lower end of the oil collar slides along the particle surface with the accumulation of oil around the contact zone.[22] The penetration depth of the collar below the level of the air-water surface, d_{CL}, increases with the value of the contact angle, θ_{ow}, and with the collar volume. When d_{CL} becomes sufficiently large, the two oil phases (in the antifoam globule and on the solution surface) coalesce with each other and globule entry is effected.[22] The necessary condition for realization of this process is

$$\theta_{ow} > 90^\circ \qquad \text{unstable asymmetric film} \tag{10.26}$$

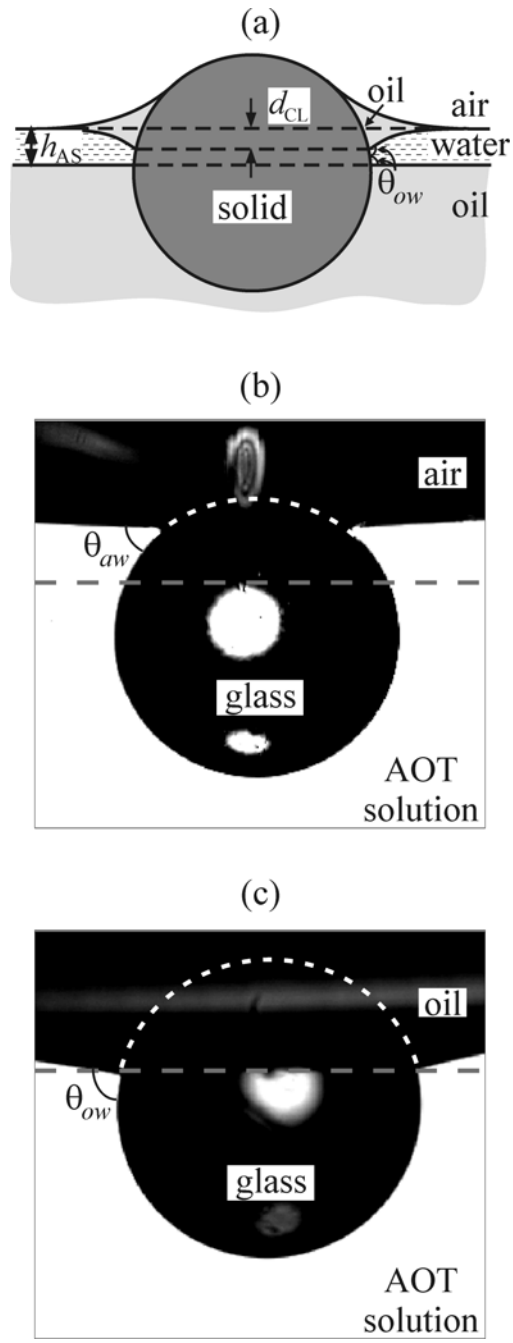

Figure 10.25. (a) Schematic presentation of the formation of an oil collar after a hydrophobic solid particle pierces the air-water surface which is covered by a layer of spread oil. (b) Photograph of a hydrophobic glass sphere attached to the air-water surface in the absence of spread oil. (c) Photograph of the same particle after spreading silicone oil on the solution surface. Note the formation of the oil collar and the subsequent change of the three-phase contact angle on the particle surface. Taken from ref. 22. The horizontal dashed lines in (b) and (c) indicate the position of the flat oil-water interface if the solid particle bridged the oil-water and air-water interfaces as shown in Figure 10.23(b).

Therefore, the condition for oil entry mediated by solid particles is condition 10.26 in the presence of spread oil, instead of condition 10.24 in the absence of spread oil. Experiments with

hydrophobized glass particles/surfaces in the presence of strong surfactants[22,26,28,55] showed that typically $\theta_{ow} \approx 130\text{-}150° > 90°$, whereas $\theta_{aw} \approx 30\text{-}70° < 90°$ above the CMC. This means that condition 10.26 is always satisfied with hydrophobic particles, whereas condition 10.24 might not be satisfied for typical detergent solutions. In the latter systems, the presence of spread oil on the foam film surfaces is an important factor for having fast antifoam action (*e.g.* the results for Triton X100 in Table 10.1).[22]

5.2.4 Effect of solid particles on lens penetration depth

Another aspect of the oil-solid particle synergy in compounds is related to the fact that the solid particles can facilitate the formation of unstable oil bridges in foam films by increasing the penetration depth, d_{PL}, of the oil lenses floating on the film surfaces. Indeed, material contact between the bottom of the lens and the opposite film surface (needed for oil bridge formation) is possible only after the film thickness becomes equal to d_{PL}, see Figure 10.26(a).

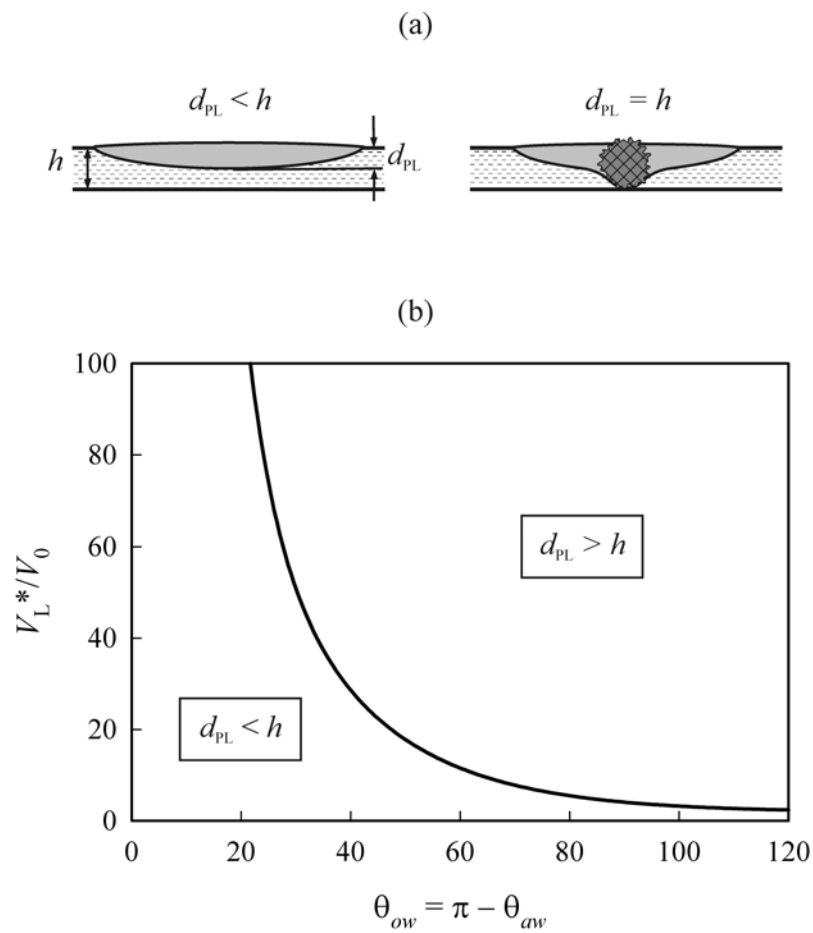

Figure 10.26. (a) Schematic presentation of the increase of the penetration depth, d_{PL}, of an oil lens due to the presence of a solid particle. (b) Plot of the calculated dimensionless volume V_L^*/V_0 of a lens with $d_{PL} = h$ in the absence of solid particles as a function of the contact angle $\theta_{ow} = (\pi - \theta_{aw})$. The scaling volume is $V_0 = \pi h^3/6$. The interfacial tensions in the calculations are typical for silicone oil: $\gamma_{oa} = 20.6$ mN m^{-1} and $\gamma_{ow} = 4.7$ mN m^{-1}.

In the absence of solid particles, d_{PL} can be very small.[10,11] This effect is illustrated in Figure 10.26(b), where we show the calculated volume, V_L*, of the oil lenses for which d_{PL} is equal to the film thickness h (for convenience V_L* is scaled with $V_0 = \pi h^3/6$). At given contact angles, lenses with volume $V_L > V_L$* "touch" the opposite surface of the foam film so that an oil bridge can be formed. Lenses with $V_L < V_L$* could not make a bridge because d_{PL} is too small. As seen from Figure 10.26(b), excessively large lenses are needed to form a bridge if $\theta_{aw} \rightarrow 180°$ (Figure 10.12), which is the typical case with silicone oils. In other words, the entry of an oil drop on one of the foam film surfaces would lead to formation of very flat lens with small d_{PL} in the absence of silica and at large contact angles θ_{aw}. The contact of such lens with the opposite film surface would require a certain period for further film thinning until the film thickness, h, becomes approximately equal to d_{PL}. In contrast, the presence of solid particles inside the lens would maintain d_{PL} comparable to the size of particle agglomerates (typically 1 to several μm), and bridge formation would become possible soon after the globule entry on the first film surface, see Figure 10.26(a).

Let us note that the presence of excess solid particles in the compound can suppress significantly its antifoam activity. Various experiments with silicone oil + silica compounds showed that bridges are always easily formed in the foam films due to the low entry barriers, see Figure 10.22 for example. However, if the silica concentration in the compound globules is above ca. 15 wt. %, they become non-deformable which is due to the formation of a relatively rigid, 3-D silica network in the compound.[23,24] Such non-deformable compound globules are unable to rupture the foam films by the bridging-stretching mechanism. The bridging-dewetting mechanism was also non-operative in the studied foaming solutions due to inappropriate contact angles.[21,23] These results confirmed the necessity to have deformable oil drops/globules for having fast antifoam action in solutions of strong surfactants at a concentration above the CMC. The effect of silica concentration on the activity of the antifoam globules is related also to the process of compound exhaustion, considered in the following sub-section.

5.3 Mechanisms of exhaustion of antifoam compounds

In this section we discuss briefly the exhaustion (deactivation) of antifoam compounds because (i) this process is a very illustrative example of the important effect on foam stability of the detailed structure/composition of the dispersed antifoam entities and (ii) the rapid compound exhaustion is a serious problem in practical applications.

5.3.1 Exhaustion and reactivation of oil-solid compounds

The process of antifoam exhaustion was illustrated in Figure 10.2 with results from the foam rise method. In Figure 10.27 we show results obtained by another method, the automatic shake test (AST), with a foaming solution of anionic surfactant containing 0.005 wt. % of silicone oil + silica compound. In this test, the foam is generated in a series of shake cycles and the defoaming

time, τ_D, is measured after each cycle.[8,12] As seen from Figure 10.27, the initial high activity of the antifoam (short τ_D) is almost constant within the first 20 cycles. Afterwards, a relatively rapid increase of τ_D is observed and the compound gets exhausted. Note that the compound exhaustion occurs only in the process of foam destruction; if the compound is kept in the same foaming solution without agitation, its antifoam activity remains virtually constant for many hours.

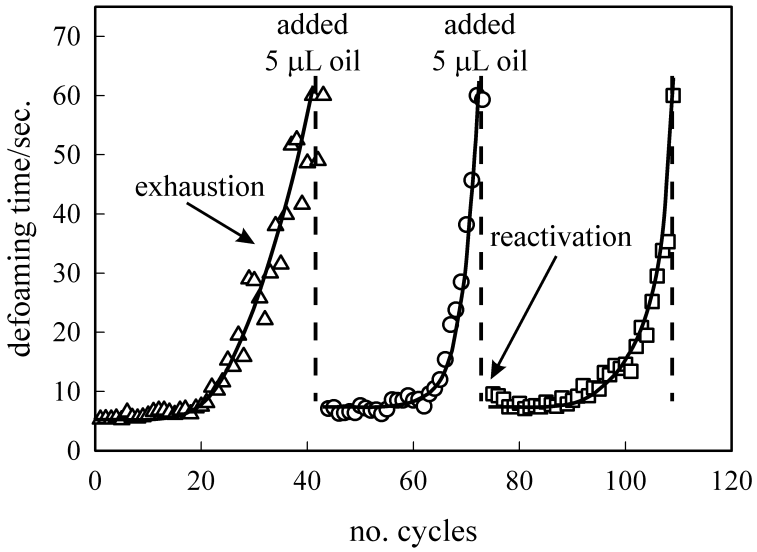

Figure 10.27. Consecutive periods of exhaustion/reactivation of 0.005 wt. % silicone oil + silica compound in an 11 mM AOT solution. An initially active antifoam (defoaming time $\tau_D > 5$ s) gradually loses its activity with the number of shaking cycles and the antifoam is considered as exhausted. The introduction of 5 μL silicone oil (0.005 wt. %) results in complete restoration of antifoam activity and τ_D falls to 5 s again. Three consecutive exhaustion profiles and two reactivations are shown. Adapted from ref. 12.

The addition of a new portion of silicone oil (deprived of silica particles) into the foaming solution containing exhausted compound leads to complete restoration of the antifoam activity, see Figure 10.27. This phenomenon is called antifoam reactivation.[12] Note, that the oil used for reactivation does not contain silica and has no antifoam activity in the timescale of interest. Hence, the reactivation process certainly involves the silica particles introduced in the original compound. As seen from Figure 10.27, the consecutive periods of exhaustion-reactivation can be repeated several times without noticeable change of the compound exhaustion profile.

5.3.2 Mechanisms of exhaustion

Several possible mechanisms were proposed in the literature to explain the compound exhaustion. In several studies,[6,28,54] a significant reduction of the size of the antifoam globules was observed upon compound exhaustion, from 5-50 μm for fresh antifoam emulsions down to 2-8 μm in exhausted ones. Hence, the authors suggested that the globule size reduction was the

main reason for the exhaustion because it resulted in lower probability for entrapment of globules in the films and/or Plateau borders. Depending on the assumed mechanism of foam destruction, the various authors compared the globule size with the film thickness or with the cross-section of the PBs. The estimates of the various timescales and of the characteristic dimensions of the foam structural elements allows one to clarify that the reported globule size reduction in these studies could be important only for slow antifoams, because it falls in the range of the cross-sections of the PBs. The observed size reduction excludes the possibility for exhaustion of the fast antifoams by this mechanism because the globule size of the exhausted compounds was sufficiently large (well above 1 μm) to allow formation of oil bridges in the early stages of the foam film thinning process. Therefore, the exhaustion of fast antifoam compounds requires a different mechanism explained below.[12,24] Only if the foam films are stabilized by polymer molecules and/or micrometer-sized solid particles (which might be the case in pulp and paper production and in some fermentation or food systems), can film thinning be much slower and the equilibrium film thickness larger than the typical cases illustrated in Figure 10.5. In such systems, the size reduction of the film-breaking antifoam globules could have a strong impact on their activity.

Alternatively, Racz *et al.*[86] suggested that the foam films are destroyed mainly by the spread oil layers, possibly containing solid particles. Hence, these authors suggested that the emulsification of spread oil, at the moment of foam film rupture, is the main reason for the antifoam exhaustion. They found by surface tension measurements that the antifoam exhaustion correlated well with the moment when the layer of spread silicone oil disappeared from the solution surface. Note, however, that most of the commercial antifoams are produced as emulsions, which means that this mechanism is incomplete and needs further development to explain the exhaustion of such pre-emulsified compounds.

Pouchelon and Araud[27] observed the formation of macroscopic white agglomerates in surfactant solutions containing over-exhausted oil + silica compounds. Infrared analysis of these agglomerates revealed that they contain silica at very high concentration (up to 17 wt. % in comparison with 2.5 wt. % in the original compound). Based on this observation, the authors suggested that the accumulation of silica into dense oil + silica agglomerates, which are inactive as antifoam entities, is the reason for the compound exhaustion.

Recent studies[12,24] showed that the exhaustion of silicone oil + silica compounds is actually a combination of two inter-related processes which occur in parallel during foam destruction. (i) The oil and silica gradually segregate into two distinct, inactive populations of antifoam globules - silica-free (deformable) and silica-enriched (non-deformable). (ii) The layer of spread oil disappears from the solution surface, see Figure 10.28. The silica-free drops are unable to enter the foam film surfaces because their entry barrier is too high (*cf.* Figure 10.22). The silica-enriched globules are able to enter the foam film surfaces and to make bridges. However these globules also cannot break the foam films in the absence of spread oil because neither the bridging-stretching mechanism (which requires deformability of the globules) nor the bridging-dewetting mechanism (which requires appropriate contact angles, unrealized in the

studied systems[24]) is operative. Since the silica-free globules do not enter the solution surface and the silica-enriched globules do not supply sufficient oil for spreading,[24] the layer of spread oil is eventually emulsified. Ultimately, the spread oil entirely disappears from the solution surface and both types of globules, silica-enriched and silica-free, become unable to destroy the foam films. The compound thus transforms into an exhausted state. These inter-related processes are schematically shown in Figure 10.28. No correlation between the size of the compound globules and their activity was established, which showed that the globule size reduction was not important in the studied systems.[12,19,24]

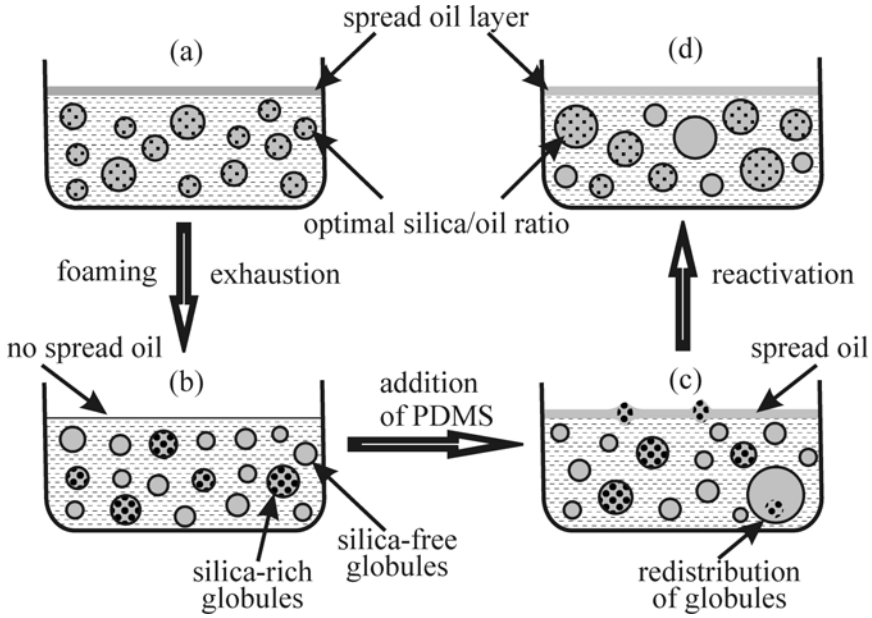

Figure 10.28. Schematic presentation of the processes of exhaustion and reactivation of silicone oil + silica antifoam. (a) Initially active antifoam contains globules of optimal oil/silica ratio and layer of spread oil is formed on the solution surface. (b) The foam destruction leads to gradual segregation of oil and silica into two inactive populations of globules (silica-free and silica-enriched); the spread oil disappears and the antifoam becomes exhausted. (c) The introduction of a new portion of oil leads to restoration of the spread oil layer and to redistribution of the silica so that active oil + silica globules are formed again; the antifoam is reactivated (d). Adapted from ref. 12.

The mechanism of compound reactivation is also illustrated in Figure 10.28 and consists of (i) restoration of the spread oil layer on the solution surface and (ii) rearrangement of the silica-enriched globules from the exhausted antifoam with fresh oil thus forming new antifoam globules with optimal silica content. In other words, the addition of oil in the system restores the configuration of the active compound with active globules and a spread oil layer.

Two possible scenarios were suggested in ref. 12 to explain the observed process of oil + silica segregation which is essential for the compound exhaustion. The first scenario is related to the bridging-stretching mechanism. In the moment of bridge stretching and rupture, very rapid expansion of the thicker oil rim at the bridge periphery (possibly containing silica) should occur, see Figure 10.29(a) and (b). This expansion could lead to a Rayleigh-type of instability and

fragmentation of the oil rim into several oil drops. Some of these drops might be devoid of silica, while the others should be silica-enriched. Thus a process of silica-oil segregation is induced, Figure 10.29(c). The subsequent emulsification of the rim fragments leads to formation of silica-enriched and silica-free globules. Note that the silica-enriched globules can again enter the solution surface and recombine with other globules and with oil lenses. Therefore, the silica-enriched globules in the exhausted samples could be even larger than the initial antifoam globules (*e.g.* the white agglomerates observed in ref. 27).

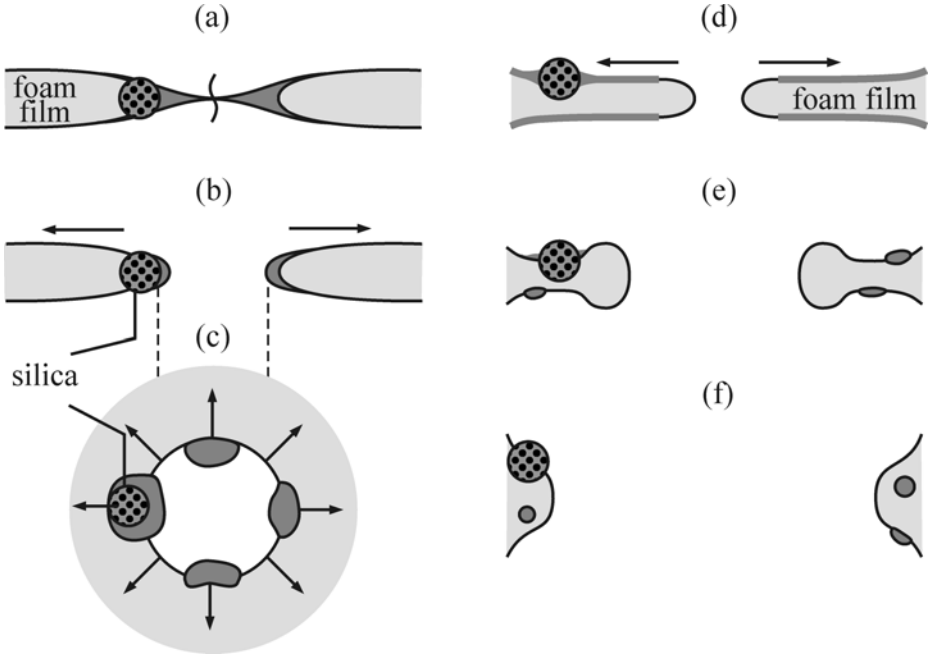

Figure 10.29. Schematic presentation of two possible mechanisms of oil + silica segregation in the process of foam film rupture. (a) and (b) After an oil bridge ruptures, the hole formed in the film rapidly expands. (c) The oil rim remaining from the bridge is stretched and fragments into several smaller oil droplets. Some of these droplets contain silica particles while others are deprived of silica. These droplets hit the adjacent Plateau borders (PBs) with high velocity and are emulsified there. (d) Part of the spread oil layer can be emulsified at the moment of foam film rupture. (e) The expansion of the hole in the film leads to rapid contraction of film surfaces and the excess of spread oil forms oil lenses which are dragged towards the PBs by the perimeter of the expanding hole. (f) The impact of these lenses with the PBs could lead to oil emulsification. Adapted from refs. 10 and 12.

The second possible scenario is illustrated in Figure 10.29(d)-(f). The foam film rupture leads to ultra-rapid contraction of the film surfaces. The oil spread on the contracting surfaces is forced to form lenses, some of them devoid of silica (Figure 10.29(e)), which are dragged by the expanding perimeter of the hole in the broken foam film. Thus, the lenses are projected with high velocity towards the PBs where they can be emulsified (Figure 10.29(f)). Subsequent cycles of globule entry → oil spreading → film rupture → emulsification of the spread oil could lead to oil + silica segregation, because the silica particles are not included in the spreading thin layers of silicone oil.

5.4 Optimal oil viscosity and globule size in antifoam compounds

The exhaustion mechanisms discussed in section 5.3 explain the fact that there is an optimum viscosity of the oils used for compound preparation.[23,25] If oil with low viscosity is used, the antifoam compound often exhibits high initial activity but exhausts rapidly due to the fast oil spreading and oil + silica segregation.[5,6,25,54] On the other hand, too viscous oils make compounds of low antifoam activity which can be explained by several factors: (i) the dispersion of the viscous compounds into numerous active globules is difficult,[25,28,54] (ii) the rate of oil spreading is low,[25,28] and (iii) the deformation of the antifoam globules which is necessary for realization of the bridging-stretching mechanism becomes too slow for efficient film rupture. Thus, an optimal oil viscosity ensuring both high initial activity and maximum durability is required.

The mechanisms discussed of foam destruction and antifoam exhaustion allow one to estimate what could be the expected optimal globule size in fast and slow antifoams. The main difficulty in making this estimate is that virtually all mechanisms imply that larger antifoam globules would be more active if the globules were considered individually. However, at fixed total weight concentration of the antifoam, the number concentration of the globules rapidly decreases with their size. Therefore, an optimal size of the globules appears, at which the globules are still very active and of sufficiently high number concentration.

The estimates of the residual foam height made in section 4.3 show that the globule diameter of the slow antifoams should be larger than the cross-section of the Plateau borders, *i.e.* at least 5 μm. Larger size would lead to faster entrapment of the globules in the PBs and hence to faster foam destruction, unless the entry barrier is too high and/or the drop number concentration is too low. With respect to the activity of fast antifoams, the optimal globule size is set by the foam film thickness, *i.e.* antifoams containing globules with diameter $d_A \approx$ 2-3 μm are expected to be very active. However, with respect to antifoam exhaustion, it is better to use bigger globules because they are more durable. The reason is that the segregation of the oil from the solid particles is faster when the initial antifoam globules are comparable in diameter to the size of the solid particles and aggregates (~ 0.1 to several μm).[24] Furthermore, significant oil + silica segregation could occur even during the fabrication of the antifoam emulsion if the antifoam globules are small. The practical experience shows that the optimal globule size is between *ca*. 5 and 30 μm, which seems to be a good compromise for having both high initial activity and reasonable durability of the antifoam emulsions.

6 Concluding remarks

Successful control of the foaming and foam stability of aqueous foams can be achieved by using appropriate hydrophobic solid particles, oil drops and oil-solid compounds. The particular mode of foam destruction depends on the type of antifoam used. It is convenient to classify the

antifoams with respect to the location where the antifoam entities enter the air-water surface and begin the foam destruction process. From this viewpoint one can distinguish:

- Fast antifoams, which destroy the foam films in the early stages of the film thinning process. The fast antifoams significantly reduce the foaminess of the surfactant solutions and destroy completely the quiescent foams in less than 1 minute after stopping the foam generation.
- Slow antifoams, which destroy the foam only after the antifoam globules are entrapped and compressed by the shrinking walls of the Plateau borders and nodes in the processes of foam drainage. Several stages in the foam evolution are observed under the action of slow antifoams, and residual long-standing foam remains in the last stage of the foam decay process.

The key factor determining whether a given active antifoam would act as fast or slow is the entry barrier, which characterizes how difficult it is for pre-dispersed antifoam globules to enter the foam film surfaces. The entry barrier was quantified by the Film Trapping Technique, and a threshold value of ≈ 15 Pa was established (in terms of critical capillary pressure leading to drop entry) which separates the fast from slow antifoams.

The characteristic features of the different types of antifoam entities can be summarized as follows:

Solid particles

- The solid particles destroy the foam films by the bridging-dewetting mechanism, which consists of two stages: (i) the solid particle comes into contact with the two opposite surfaces of the foam film making a solid bridge between them and (ii) the liquid dewets the particle and the foam film gets perforated at the particle surface.
- The antifoam efficiency of solid particles depends mainly on their hydrophobicity, shape and size. For complete dewetting of solid particles with smooth convex surface (spheres, ellipsoids), the three phase contact angle air-water-solid should be higher than 90°. Particles with sharp edges (cubes, prisms, cones, needles, star-shaped and irregularly shaped particles) can destroy the foam films even when their contact angles are as low as 30-40° if the particles are properly oriented in the foam film. In addition, the presence of sharp edges strongly facilitates particle entry and bridge formation. The size of the solid particles becomes an important issue for their antifoam action only if they are too small (with radius below *ca.*1 μm).
- If the solid particles are too hydrophilic to act as antifoams, they can strongly enhance the foam stability by several mechanisms; stabilizing very thick equilibrium foam films, decelerating the water drainage from the foam or arresting the bubble coarsening through gas diffusion across the films.

Oil drops

- Oil drops can destroy foams by various mechanisms; bridging-stretching, bridging-dewetting and several mechanisms related to oil spreading.
- The necessary requirements for having active antifoams depend on the particular mechanism of foam destruction. For the bridging mechanisms, the bridging coefficient, B, should be positive to ensure unstable bridges. For the mechanisms related to oil spreading, the initial spreading coefficient S_{IN} should be positive to ensure oil spreading at least as a thin layer.
- The antifoam efficiency of oil drops correlates well with their entry barrier. If the entry barrier is below the threshold value of 15 Pa, the oil drops behave as fast antifoams and break the foam films by the bridging mechanisms (if $B > 0$). If the entry barrier is higher, the oil drops destroy the foam as slow antifoams by bridging or spreading mechanisms after drop entry in the Plateau borders. In typical surfactant solutions at a concentration above the CMC, the oil drops usually behave as slow antifoams because their entry barrier is above 15 Pa.
- The drop entry barrier depends on various factors, such as the presence of co-surfactant and electrolyte, presence of solid particles, oil drop size, chemical nature of the oil which can be used for efficient control of the antifoam effect to achieve a desired result (fast foam destruction or foam boosting).

Oil-solid compounds

- The oil-solid compounds with large excess of oil can destroy the foam by the same mechanisms as the oil drops. The main difference between compounds and oil drops is that the compound globules usually have a much lower entry barrier (due to the pin effect of the solid particles), which allows them to act as fast antifoams even in surfactant solutions of high concentration.
- The strong synergistic effect between oil and solid particles in the antifoam compounds is due to the complementary roles of the two components. The main role of the solid particles is to destabilize the asymmetric oil-water-air films, facilitating in this way the oil drop entry (pin-effect) and in some systems to increase the penetration depth of the oil lenses. The main role of the oil is to ensure deformability of the compound globules and to spread on the solution surface. The globule deformability is an important pre-requisite for foam film rupture by the bridging-stretching mechanism and in many cases by the bridging-dewetting mechanism. Oil spreading facilitates the entry of the antifoam globules and the foam film rupture. In some systems related to mineral flotation (when the solid particles are in excess and no strong surfactants are used), the oil can coat the particle surface rendering it more hydrophobic.
- The exhaustion (deactivation) of the fast oil-solid compounds is mainly due to the segregation of the oil and solid particles in the course of foam destruction into two inactive populations of globules - particle-free and particle-enriched. The particle-free globules are unable to enter the foam film surfaces due to their high entry barrier, whereas the particle-enriched globules are non-deformable and, hence, cannot break the foam films.

At the end, let us note that the short review presented cannot cover all aspects of the mechanisms of antifoam action. The systems and processes involved are so complex that new experimental results can always surprise us and require further upgrade of the various mechanisms outlined above. One class of systems, which is still not very well understood and deserves more systematic investigation is the antifoams used for non-aqueous foams. The recent advance in the application of new experimental methods for studying the modes of antifoam action and the new ways for synthesis of various solid particles with desired properties suggest that the antifoam research area will continue to develop rapidly.

Acknowledgements

The authors are grateful to Dr. S. Tcholakova from Sofia University for the numerous useful discussions and for a critical reading and help in the preparation of the manuscript. Our colleagues from the Laboratory in Sofia, who contributed in many different ways to the original studies (see refs. 10-26), are gratefully acknowledged for their quality efforts.

References

1. *Foams: Theory, Measurements and Applications*, eds. R.K. Prud'homme and S.A. Khan, Surfactant Science Series, Vol. 57, Marcel Dekker, New York, 1996.
2. A. Prins, in *Food Emulsions and Foams*, ed. E. Dickinson, Royal Society of Chemistry Special Publication, Vol. 58, Cambridge, 1986, p. 30.
3. P.R. Garrett, in *Defoaming: Theory and Industrial Applications*, ed. P.R. Garrett, Marcel Dekker, New York, 1993, Chapter 1.
4. *Defoaming: Theory and Industrial Applications*, Vol. 45, ed. P.R. Garrett, Surfactant Science Series, Marcel Dekker, New York, 1993.
5. D.T. Wasan and S.P. Christiano, in *Handbook of Surface and Colloid Chemistry*, ed. K. Birdi, CRC Press, New York, 1997, Chapter 6.
6. D.T. Wasan, K. Koczo and A.D. Nikolov, in *Foams: Fundamentals and Applications in Petroleum Industry*, ed. L.L. Schramm, ACS Symposium Series No. 242, ACS, New York, 1994, Chapter 2.
7. D. Exerowa and P.M. Kruglyakov, *Foams and Foam Films: Theory, Experiment, Application*, Elsevier, Amsterdam, 1998.
8. N.D. Denkov, *Langmuir*, **20** (2004), 9463.
9. S. Ross and G. Nishioka, in *Emulsion, Latices and Dispersions*, eds. P. Becher and M.N. Yudenfrend, Marcel Dekker, New York, 1978.
10. N.D. Denkov, P. Cooper and J-Y. Martin, *Langmuir*, **15** (1999), 8514.

11. N.D. Denkov, *Langmuir*, **15** (1999), 8530.
12. N.D. Denkov, K. Marinova, H. Hristova, A. Hadjiiski and P. Cooper, *Langmuir*, **16** (2000), 2515.
13. N.D. Denkov and K.G. Marinova, in *Proceedings of 3rd Eurofoam Conference*, Verlag MIT Publishing, Bremen, 2000, pp. 199.
14. E.S. Basheva, D. Ganchev, N.D. Denkov, K. Kasuga, N. Satoh and K. Tsujii, *Langmuir*, **16** (2000), 1000.
15. E.S. Basheva, S. Stoyanov, N.D. Denkov, K. Kasuga, N. Satoh and K. Tsujii, *Langmuir*, **17** (2001), 969.
16. A. Hadjiiski, N.D. Denkov, S. Tcholakova and I.B. Ivanov, in *Adsorption and Aggregation of Surfactants in Solution*, eds. K. Mittal and D. Shah, Marcel Dekker, New York, 2002, pp. 465.
17. L. Arnaudov, N.D. Denkov, I. Surcheva, P. Durbut, G. Broze and A. Mehreteab, *Langmuir*, **17** (2001), 6999.
18. A. Hadjiiski, S. Tcholakova, N.D. Denkov, P. Durbut, G. Broze and A. Mehreteab, *Langmuir*, **17** (2001), 7011.
19. K.G. Marinova and N.D. Denkov, *Langmuir*, **17** (2001), 2426.
20. N.D. Denkov, K. Marinova, S. Tcholakova and M. Deruelle, in *Proceedings 3rd World Congress on Emulsions*, September 2002, Lyon, paper 1-D-199.
21. K.G. Marinova, N.D. Denkov, P. Branlard, Y. Giraud and M. Deruelle, *Langmuir*, **18** (2002), 3399.
22. N.D. Denkov, S. Tcholakova, K.G. Marinova and A. Hadjiiski, *Langmuir*, **18** (2002), 5810.
23. K.G. Marinova, N.D. Denkov, S. Tcholakova and M. Deruelle, *Langmuir*, **18** (2002), 8761.
24. K.G. Marinova, S. Tcholakova, N.D. Denkov, S. Roussev and M. Deruelle, *Langmuir*, **19** (2003), 3084.
25. N.D. Denkov, S. Tcholakova, K.G. Marinova, N. Christov, N. Vankova and M. Deruelle, in preparation.
26. K.G. Marinova, D. Christova, S. Tcholakova, E. Efremov and N.D. Denkov, *Langmuir*, **21** (2005) 11729.
27. A. Pouchelon and C. Araud, *J. Disp. Sci. Technol.,* **14** (1993), 447.
28. V. Bergeron, P. Cooper, C. Fischer, J. Giermanska-Kahn, D. Langevin and A. Pouchelon, *Colloids Surf. A,* **122** (1997), 103.
29. T.A. Koretskaya, *Koll. Zeit.,* **39** (1977), 71.
30. A. Bonfillon-Colin and D. Langevin, *Langmuir*, **13** (1997), 599.
31. R. Chaisalee, S. Soontravanich, N. Yanumet and J.F. Scamehorn, *J. Surf. Det.,* **6** (2003), 345.
32. P.R. Garrett, J. Davis and H.M.Rendall, *Colloids Surf. A*, **85** (1994), 159.
33. D. Weaire and S. Hutzler, *The Physics of Foams*, Clarendon Press, Oxford, 1999.

34. G. Narsimhan and E. Ruckenstein, in *Foams: Theory, Measurements, and Applications*, eds. R.K. Prud'homme and S.A. Khan, Surfactant Science Series, Vol. 57, Marcel Dekker, New York, 1996, Chapter 2.
35. P.A. Kralchevsky, K.D. Danov and N.D. Denkov, in *Handbook of Surface and Colloid Chemistry*, ed. K.S. Birdi, 2nd Expanded and Updated Edition, CRC Press, New York, 2002, Chapter 5.
36. *Thin Liquid Films: Fundamentals and Applications*, ed. I.B. Ivanov, Marcel Dekker, New York, 1988.
37. P.A. Kralchevsky and K. Nagayama, *Particles at Fluid Interfaces and Membranes*, Elsevier, Amsterdam, 2001.
38. N.D. Denkov, H. Yoshimura and K. Nagayama, *Ultramicroscopy*, **65** (1996), 147.
39. K.P. Velikov, F. Durst and O.D. Velev, *Langmuir*, **14** (1998), 1148.
40. R.G. Alargova, D.S. Warhadpande, V.N. Paunov and O.D. Velev, *Langmuir*, **20** (2004), 10371.
41. A.D. Nikolov, D.T. Wasan, P.A. Kralchevsky and I.B. Ivanov, *J. Colloid Interface Sci.*, **133** (1989), 1 and 13.
42. V. Bergeron and C.J. Radke, *Langmuir*, **8** (1992), 3020.
43. I.B. Ivanov and D.S. Dimitrov, in *Thin Liquid Films: Fundamentals and Applications*, ed. I.B. Ivanov, Marcel Dekker, New York, 1988, Chapter 7.
44. T.T. Traykov, E.D. Manev and I.B. Ivanov, *Int. J. Multiphase Flow*, **3** (1977), 485.
45. E. Manev, R. Tsekov and B. Radoev, *J. Disp. Sci. Technol.*, **18** (1997), 769.
46. J.E. Coons, P.J. Halley, S.A. McGlashan and T. Tran-Cong, *Adv. Colloid Interface Sci.*, **105** (2003), 3.
47. D. Weaire, S. Hutzler, G. Verbist and E. Peters, *Adv. Chem. Phys.,* **102** (1997), 315.
48. S.J. Cox, D. Weaire, S. Hutzler, J. Murphy, R. Phelan and G. Verbist, *Proc. Roy. Soc. London A,* **456** (2000), 2441.
49. S.A. Koehler, S. Hilgenfeldt and H.A. Stone, *Langmuir*, **16** (2000), 6327.
50. A. Saint-Jalmes, M.U. Vera and D.J. Durian, *Europhys. Lett.*, **50** (2000), 695.
51. A. Saint-Jalmes and D. Langevin, *J. Phys.: Condens. Matter*, **14** (2002), 9397.
52. W.W. Mullins, *J. Appl. Phys.,* **59** (1986), 1341.
53. S. Hilgenfeldt, S. Koehler and H.A. Stone, *Phys. Rev. Lett.*, **86** (2001), 4704.
54. K. Koczo, J.K. Koczone and D. Wasan, *J. Colloid Interface Sci.*, **166** (1994), 225.
55. G.C. Frye and J.C. Berg, *J. Colloid Interface Sci.*, **127** (1989), 222.
56. K. Roberts, C. Axberg and R. Österlund, *J. Colloid Interface Sci.*, **62** (1977), 264.
57. P.R. Garrett, *J. Colloid Interface Sci.*, **69** (1979), 107.
58. A. Dippenaar, *Int. J. Min. Proc.,* **9** (1982), 1.
59. R. Aveyard, P. Cooper, P.D.I. Fletcher and C.E. Rutherford, *Langmuir*, **9** (1993), 604.

60. R. Aveyard, B.P. Binks, P.D.I. Fletcher, T.G. Peck and C.E. Rutherford, *Adv. Colloid Interface Sci.*, **48** (1994), 93.
61. R. Aveyard and J.H. Clint, *J. Chem. Soc. Faraday Trans.*, **91** (1995), 2681.
62. R. Aveyard, B.D. Beake and J.H. Clint, *J. Chem. Soc. Faraday Trans.*, **92** (1996), 4271.
63. G.C. Frye and J.C. Berg, *J. Colloid Interface Sci.*, **130** (1989), 54.
64. R.D. Kulkarni, E.D. Goddard and B. Kanner, *Ind. Eng. Chem. Fund.,* **16** (1977), 472.
65. R.D. Kulkarni, E.D. Goddard and B. Kanner, *J. Colloid Interface Sci.*, **59** (1977), 468.
66. K. Golemanov, S. Tcholakova, P. A. Kralchevsky, K. P. Ananthapadmanabhan, and A. Lips, *Langmuir* **22** (2006) 4968.
67. B.V. Derjaguin, *Theory of Stability of Colloids and Thin Liquid Films*, Plenum, New York, 1989.
68. H. Zhang, C.A. Miller, P.R. Garrett, and K.H. Raney, *J. Colloid Interface Sci.*, **279** (2004), 539.
69. P.R. Garrett, *J. Colloid Interface Sci.*, **76** (1980), 587.
70. R. Aveyard, B.P. Binks, P.D.I. Fletcher, T-G. Peck and P.R. Garrett, *J. Chem. Soc. Faraday Trans.*, **89** (1993), 4313.
71. W.D. Harkins, *J. Chem. Phys.*, **9 (**1941), 552.
72. S. Ross, *J. Phys. Colloid Chem.*, **54** (1950), 429.
73. P.M. Kruglyakov and T.A. Koretskaya, *Koll. Zeit.,* **36 (**1974), 627.
74. K. Koczo, L. Lobo and D.T. Wasan, *J. Colloid Interface Sci.*, **150** (1992), 492.
75. B.K. Jha, S.P. Christiano and D.O. Shah, *Langmuir*, **16** (2000), 9947.
76. V. Bergeron, M.E. Fagan and C.J. Radke, *Langmuir*, **9** (1993), 1704.
77. P.M. Kruglyakov and N.G. Vilkova, *Colloids Surf. A,* **156** (1999), 475.
78. B.P Binks, P.D.I. Fletcher and M.D. Haynes, *Colloids Surf. A,* **216** (2003), 1.
79. B. Dimitrova, I.B. Ivanov and E. Nakache, *J. Disp. Sci. Technol.,* **9** (1988), 321.
80. K. Danov, I.B. Ivanov, Z.Z. Zapryanov, E. Nakache and S. Raharimalala, in *Synergetics, Order and Chaos*, ed. M.G. Velarde, World Scientific, London, 1988, p. 178.
81. D.S. Valkovska, P.A. Kralchevsky, K.D. Danov, G. Broze and A. Mehreteab, *Langmuir*, **16** (2000), 8892.
82. M. Aronson, *Langmuir*, **2** (1986**)**, 653.
83. P.R. Garrett and P.R. Moor, *J. Colloid Interface Sci.*, **159** (1993), 214.
84. H. Zhang, C.A. Miller, P.R. Garrett and K.H. Raney, *J. Colloid Interface Sci.*, **263** (2003), 633.
85. R.E. Patterson, *Colloids Surf. A,* **74** (1993), 115.
86. G. Racz, K. Koczo and D.T. Wasan, *J. Colloid Interface Sci.*, **181** (1996), 124.